

Dynamical Properties of a Two-gene Network with Hysteresis

Qin Shu

shuq@email.arizona.edu

Ricardo G. Sanfelice

sricardo@u.arizona.edu

arXiv:1402.0130v1 [cs.LG] 1 Feb 2014

October 30, 2018

Technical Report
Hybrid Dynamics and Control Laboratory
Department of Aerospace and Mechanical Engineering
University of Arizona, Tucson

Technical Report No. UA/AME/HDC-2014-001. **Status:** NOT PUBLISHED. **Readers of this material have the responsibility to inform all of the authors promptly if they wish to reuse, modify, correct, publish, or distribute any portion of this report.**

<http://www.u.arizona.edu/~sricardo/index.php?n=Main.TechnicalReports>

Dynamical Properties of a Two-gene Network with Hysteresis

Qin Shu and Ricardo G. Sanfelice*

October 30, 2018

Abstract

A mathematical model for a two-gene regulatory network is derived and several of their properties analyzed. Due to the presence of mixed continuous/discrete dynamics and hysteresis, we employ a hybrid systems model to capture the dynamics of the system. The proposed model incorporates binary hysteresis with different thresholds capturing the interaction between the genes. We analyze properties of the solutions and asymptotic stability of equilibria in the system as a function of its parameters. Our analysis reveals the presence of limit cycles for a certain range of parameters, behavior that is associated with hysteresis. The set of points defining the limit cycle is characterized and its asymptotic stability properties are studied. Furthermore, the stability property of the limit cycle is robust to small perturbations. Numerical simulations are presented to illustrate the results.

*Q. Shu and R. G. Sanfelice are with the Department of Aerospace and Mechanical Engineering, University of Arizona 1130 N. Mountain Ave, AZ 85721. Email: shuq@email.arizona.edu, sricardo@u.arizona.edu. This research has been partially supported by the National Science Foundation under CAREER Grant no. ECS-1150306 and by the Air Force Office of Scientific Research under Grant no. FA9550-12-1-0366.

Contents

1	Introduction	3
1.1	Mathematical modeling of genetic regulatory networks	3
1.2	The role of hysteresis in genetic regulatory networks	3
1.3	Contributions and organization of the paper	3
2	A Hybrid Model for Genetic Networks w/Hysteresis	4
2.1	Introduction to Hybrid System Modeling	6
2.2	Modeling of a Two-Gene Network	7
3	Dynamical Properties of the Two-Gene Hybrid System Model	10
3.1	Existence of solutions	10
3.2	Characterization of equilibria	11
3.3	Stability analysis	15
3.3.1	Asymptotic stability of isolated equilibrium points	15
3.3.2	Stability properties of the limit cycle	15
3.4	Robustness properties	20
4	Numerical results	21
4.1	Isolated equilibrium points in Table 1	21
4.1.1	Case 1 of Table 1	21
4.1.2	Case 2 of Table 1	22
4.1.3	Case 3 of Table 1	23
4.1.4	Case 4 of Table 1	24
4.2	Equilibrium set S	25
5	Conclusion	31
A		34
A.1	Proof of Proposition 3.3	34
A.2	Proof of Proposition 3.1	40
A.3	Proof of Proposition 3.5	44
A.4	Proof of Proposition 3.6	52

1 Introduction

1.1 Mathematical modeling of genetic regulatory networks

In recent years, the development of advanced experimental techniques in molecular biology has led to a growing interest in mathematical modeling methods for the study of genetic regulatory networks; see [1] for a literature review. A number of gene regulatory network models have been proposed to capture their main properties [2], [3], [4], [5], [6], [7], [8]. Boolean models capture the dynamics of the discrete switch in genetic networks. As introduced by Glass and Kauffman in [3], Boolean regulation functions, typically modeled as sigmoidal or step functions, can be combined with linear system models to enforce certain logic rules. The properties of such a class of piecewise linear models have been studied in the mathematical biology literature, e.g., [4, 5, 2, 6]. Snoussi presented a discrete mapping approach in [4] to study the qualitative properties of the dynamics of genetic regulatory networks. In this work, the properties of the discrete mapping were studied to determine stable isolated steady states as well as limit cycles. In [5], Gouzé and Sari employ the concept of Filippov solution to study piecewise linear models of genetic regulatory networks with discontinuities occurring on hyperplanes defined by thresholds on the variables. Chaves and coauthors [2] studied the robustness of Boolean models of gene control networks. de Jong and coauthors [6] presented a method for qualitative simulation of genetic regulatory networks based on the piecewise linear model of [3]. Genetic regulatory networks with continuous dynamics coupled with switching can be written as a hybrid system. In [7] and [8], the authors apply hybrid systems tools to model a variety of cell biology problems. More recently, hybrid models have been used in [9] for the study of molecular interactions. It is important to note that hysteresis behavior, which is typically present in genetic regulatory networks, has not been considered in the models mentioned above.

1.2 The role of hysteresis in genetic regulatory networks

Hysteresis is an important phenomenon in genetic regulatory networks. It is characterized by behavior in which, for instance, once a gene has been inhibited due to the concentration of cellular protein reaching a particularly low value, a higher value of cellular protein concentration is required to express it. In his survey paper on the impact of genetic modeling on tumorigenesis and drug discovery [10], Huang stated that *“hysteresis is a feature that a synthetic model has to capture.”* Through experiments, Das and coauthors [11] demonstrated the existence of hysteresis in lymphoid cells and the interaction of continuous evolution of some cellular proteins. Hysteresis was also found to be present in mammalian genetic regulatory networks; see, e.g., [12, 13]. More importantly, it has been observed that hysteresis is a key mechanism contributing to oscillatory behavior in computational biological models [14], [15]. On the other hand, it is well known that hysteresis is one of the key factors that makes a system robust to noise and parametric uncertainties [16], [17].

1.3 Contributions and organization of the paper

Our work is motivated by the following facts:

1. *Piecewise linear models do not incorporate hysteresis, although it plays a key role in the dynamics of genetic regulatory networks. In fact, as we establish in this paper, hysteresis leads to oscillatory, robust behavior in two-gene networks.*
2. *The discontinuities introduced by the Boolean regulation functions yield a non-smooth dynamical system, for which classical analysis tools cannot be applied to study existence of solutions, stability, robustness, etc.*

Motivated by these two limitations, we propose a hybrid system model that captures both continuous and discrete dynamics of genetic regulatory networks with hysteresis behavior. We combine the methodology of piecewise linear modeling of genetic regulatory networks with the framework of hybrid dynamical systems in [18], and construct a hybrid system model for a genetic network with two genes. Our model incorporates hysteresis explicitly, which we found leads to limit cycles. We prove existence of solutions and compute the equilibrium points in terms of parameters for the system. We analyze the stability of the isolated equilibrium points and determined conditions under which a limit cycle exists. It is found that hysteresis is the key mechanism leading to hysteresis, as without hysteresis, the limit cycle converges to an isolated equilibrium point (cf. [4]). The stability of the limit cycle is established using a novel approach consisting of measuring distance between solutions of hybrid systems (rather than the distance to the limit cycle as in classical continuous-time systems). Moreover, we show that the asymptotic stability of the limit cycle is robust to small perturbations.

The remainder of this paper is organized as follows. In Section 2, a mathematical framework of hybrid dynamical system is introduced and then applied to model a two-gene network. The analysis of existence of solutions, stability, and robustness are presented in Section 3. Section 4 presents simulations validating our results.

2 A Hybrid Systems Model for Genetic Regulatory Networks with Hysteresis

Models of genetic regulatory networks given by piecewise-linear differential equations have been proposed in [8], [19]. Such models take the form ¹

$$\dot{x} = f(x) - \gamma x, \quad x \geq 0, \quad (1)$$

where $x = [x_1, x_2, \dots, x_n]^\top$ and x_i represents the concentration of the protein in the i -th cell, $f = [f_1, f_2, \dots, f_n]^\top$ is a function, $\gamma = [\gamma_1, \gamma_2, \dots, \gamma_n]^\top$ is a vector of constants, and $1 \leq i \leq n$. For each i , f_i is a function representing the rate of synthesis, while γ_i represents the degradation rate constant of the protein. The function f_i is typically defined as the linear combination $f_i(x) = \sum_{\ell \in L} k_{i\ell} b_{i\ell}(x)$ where $k_{i\ell}$ is the nonzero and nonnegative growth rate constants, $b_{i\ell}$ is a Boolean regulation function that describes the gene regulation logic, and $L = \{1, 2, \dots, n\}$ is the set of indices of regulation functions.

The modeling strategy for the Boolean regulation functions $b_{i\ell}$ is a key element that captures the behavior of a particular genetic regulatory network. A major feature of a

¹The notation $x \geq 0$ is equivalent to $x_i \geq 0$ for each i .

genetic regulatory network is the presence of threshold-like relationships between the system variables, i.e., if a variable x_i is above (or below) a certain level, it could cause little or no effect on another variable x_j , whereas if x_i is below (or above) this certain value, the effect on x_j would become more significant (for example, it may increase the value of x_j or inhibit the growth of the value of x_j). Boolean regulation functions can be modeled by sigmoidal or step functions, an approach that was first proposed by Glass and Kauffmann [3]. When modeling as a step function, the functions $b_{i\ell}$ are given by the combination (linear or nonlinear) of

$$s^+(x_i, \theta) = \begin{cases} 1 & \text{if } x_i \geq \theta \\ 0 & \text{if } x_i < \theta \end{cases}, \quad s^-(x_i, \theta) = 1 - s^+(x_i, \theta), \quad (2)$$

where $s^+(x_i, \theta)$ represents the logic for gene expression when the protein concentration exceeds a threshold θ , while $s^-(x_i, \theta)$ represents the logic for gene inhibition.

To illustrate this modeling approach, let us consider the genetic regulatory network shown in Figure 1. Genes a and b encode proteins A and B , respectively. When the concentration of protein A is below certain threshold, it will inhibit gene b . Similarly, protein B inhibits gene a when the concentration of protein B is above certain threshold. In this way, a set of piecewise-linear differential equations representing the behavior in Figure 1 is given by

$$\dot{x}_1 = k_1 s^-(x_2, \theta_2) - \gamma_1 x_1, \quad \dot{x}_2 = k_2 s^+(x_1, \theta_1) - \gamma_2 x_2, \quad (3)$$

where x_1 is representing the concentration of protein A , while x_2 is the concentration of protein B . The constants θ_1, θ_2 are the thresholds associated with concentrations of protein A and B , respectively.

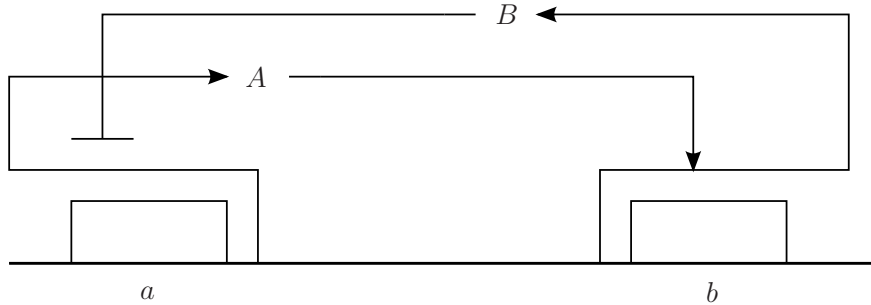


Figure 1: A genetic regulatory network of two genes (a and b), each encoding for a protein (A and B). Lines ending in arrows represent genetic expression triggers, while lines ending in flatheads refer to genetic inhibition triggers.

In this model, gene a is expressed at a rate k_1 when x_2 is below the threshold θ_2 . Similarly, gene b is expressed at a rate k_2 when x_1 is above the threshold θ_1 . Degradations of both proteins are assumed to be proportional to their own concentrations, a mechanism that is captured by $-\gamma_1 x_1$ and $-\gamma_2 x_2$, respectively.

Note that the model in (3) capturing the interaction between gene a and gene b does not incorporate binary hysteresis. Furthermore, due to the discontinuities introduced by the Boolean regulation functions, it is not straightforward to argue that solutions to (3) exist

from every initial value of x . In order to overcome such limitations, we propose a hybrid system with hysteresis for this two gene genetic regulatory network, to which hybrid systems tools for analysis of existence of solutions and asymptotic stability can be applied.

2.1 Introduction to Hybrid System Modeling

Following [18] and [20], a hybrid system in this paper is defined by four objects:

- A set $C \subset \mathbb{R}^n$, called the *flow set*.
- A set $D \subset \mathbb{R}^n$, called the *jump set*.
- A single-valued mapping $F: \mathbb{R}^n \rightarrow \mathbb{R}^n$, called the *flow map*.
- A set-valued mapping $G: \mathbb{R}^n \rightrightarrows \mathbb{R}^n$, called the *jump map*.

The flow map F defines the continuous dynamics on the flow set C , while the jump map G defines the discrete dynamics or jumps on the jump set D . These objects are referred to as the data of the hybrid system \mathcal{H} . Then, defining $z \in \mathbb{R}^n$ to be the state of the system, \mathcal{H} can be written in the compact form

$$\mathcal{H}: \begin{cases} \dot{z} = F(z) & z \in C \\ z^+ \in G(z) & z \in D \end{cases}$$

Solutions to hybrid systems are given by hybrid arcs which are trajectories defined on hybrid time domains.

Definition 2.1 (hybrid time domain) *A set E is a hybrid time domain if for all $(T, J) \in E$, $E \cap ([0, T] \times \{0, 1, \dots, J\})$ is a compact hybrid time domain; that is, it can be written as $\cup_{j=0}^{J-1} ([t_j, t_{j+1}], j)$ for some finite sequence of times $0 \leq t_0 \leq t_1 \leq \dots \leq t_J$.*

Definition 2.2 (hybrid arc) *A hybrid arc ϕ is a function that takes values from \mathbb{R}^n , is defined on a hybrid time domain $\text{dom } \phi$, and is such that $t \mapsto \phi(t, j)$ is locally absolutely continuous for every j , $(t, j) \in \text{dom } \phi$.*

Hybrid time domains impose a specific structure on the domains of solutions to hybrid systems. In simple words, solutions to \mathcal{H} are defined on intervals of flow $[t_j, t_{j+1}]$ indexed by the jump time j when $t_{j+1} > t_j$. Hybrid arcs specify the functions that define solutions to hybrid systems when the following conditions are satisfied. We refer the reader to [20, 18] for more details on the definition of solutions to hybrid systems.

Definition 2.3 (solution) *A hybrid arc ϕ is a solution to the hybrid system \mathcal{H} if $\phi(0, 0) \in \overline{C} \cup D$ and*

(S1) *For all $j \in \mathbb{N} := \{0, 1, 2, \dots\}$ and almost all t such that $(t, j) \in \text{dom } \phi$,*

$$\phi(t, j) \in C, \quad \dot{\phi}(t, j) = F(\phi(t, j))$$

(S2) *For all $(t, j) \in \text{dom } \phi$ such that $(t, j + 1) \in \text{dom } \phi$,*

$$\phi(t, j) \in D, \quad \phi(t, j + 1) \in G(\phi(t, j))$$

Solutions to hybrid systems are classified as follows:

- A solution ϕ to \mathcal{H} is said to be nontrivial if $\text{dom } \phi$ contains at least two points.
- A solution ϕ to \mathcal{H} is said to be complete if $\text{dom } \phi$ is unbounded.
- A solution ϕ to \mathcal{H} is said to be Zeno if it is complete and the projection of $\text{dom } \phi$ onto $\mathbb{R}_{\geq 0}^n$ is bounded.
- A solution ϕ to \mathcal{H} is said to be maximal if there does not exist another solution φ to \mathcal{H} such that $\text{dom } \varphi$ is a proper subset of $\text{dom } \phi$, and $\varphi(t, j) = \phi(t, j)$ for all $(t, j) \in \text{dom } \phi$.

The reader is referred to [18] and [20] for more details on this hybrid system framework.

2.2 Modeling of a Two-Gene Network

To model the genetic network in (3) as a hybrid system \mathcal{H} , two discrete logic variables, q_1 and q_2 , are introduced. The dynamics of these variables depend on the thresholds, θ_1 and θ_2 , respectively. As one of our goals is to introduce binary hysteresis in the model in (3), we define hysteresis level constants h_1 and h_2 associated with gene a and gene b , respectively. In this way, q_i is governed by dynamics such that the evolution in Figure 2 holds.

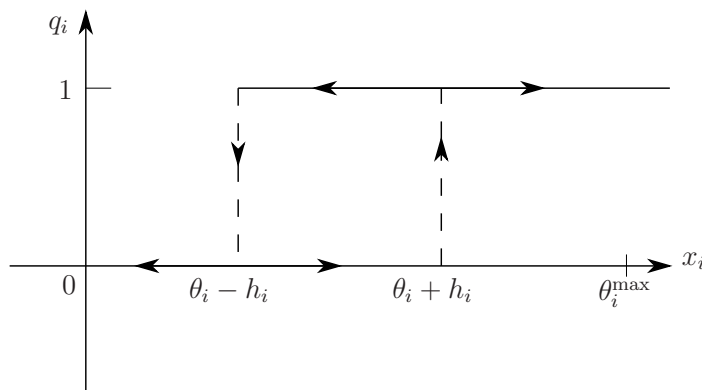


Figure 2: *The update mechanism of q_i as a function of x_i and previous values of q_i .*

The state of the hybrid system is defined as

$$z = [x_1, x_2, q_1, q_2]^\top,$$

where $z \in \mathcal{Z} := \mathbb{R}_{\geq 0}^2 \times \{0, 1\}^2$; x_1, x_2 are (nonnegative) continuous states representing protein concentrations; and q_1, q_2 are discrete variables. Here, $\mathbb{R}_{\geq 0} := [0, +\infty)$. We specify constants θ_1 and θ_2 , usually inferred from biological data, satisfying $0 < \theta_1 < \theta_1^{\max}, 0 < \theta_2 < \theta_2^{\max}$, where θ_1^{\max} and θ_2^{\max} are the maximal value of the concentration of protein A and of the protein B , respectively.

To define the continuous dynamics of the hybrid system capturing the evolution of (3), we rewrite the piecewise-linear differential equation (3) by replacing the s^+ term with the

logic variables q_i , and the s^- term with the complement of the logic variable q_i , i.e., $1 - q_i$. Note that the discrete logic variables q_i only change at jumps, i.e., they are constants during flows. Then, $\dot{q}_i = 0$. In this way, the continuous dynamics are governed by the differential equation

$$\dot{x}_1 = k_1(1 - q_2) - \gamma_1 x_1, \quad \dot{x}_2 = k_2 q_1 - \gamma_2 x_2, \quad \dot{q}_1 = \dot{q}_2 = 0,$$

from where we obtain the flow map

$$F(z) = \begin{bmatrix} k_1(1 - q_2) - \gamma_1 x_1 \\ k_2 q_1 - \gamma_2 x_2 \\ 0 \\ 0 \end{bmatrix}. \quad (4)$$

Now, we describe the discrete update of the state vector z , i.e., we define G and D . To illustrate this construction, we explain how to model the mechanism in Figure 2 for q_1 . When

$$q_1 = 0 \quad \text{and} \quad x_1 = \theta_1 + h_1$$

the state q_1 is updated to 1. We write this update law as

$$q_1^+ = 1.$$

When

$$q_1 = 1 \quad \text{and} \quad x_1 = \theta_1 - h_1,$$

then the state q_1 is updated to 0, i.e.,

$$q_1^+ = 0.$$

It follows that the mechanism of q_1 in Figure 2 can be captured by triggering jumps when the components of z satisfy

$$q_1 = 0, \quad x_1 = \theta_1 + h_1 \quad \text{or} \quad q_1 = 1, \quad x_1 = \theta_1 - h_1$$

Note that the update mechanism for q_2 is similar to that of q_1 just discussed.

We can define the flow and jump sets in a compact form by defining functions

$$\eta_1(x_1, q_1) := (2q_1 - 1)(-x_1 + \theta_1 + (1 - 2q_1)h_1)$$

$$\eta_2(x_2, q_2) := (2q_2 - 1)(-x_2 + \theta_2 + (1 - 2q_2)h_2).$$

In this way, the flow set is given by

$$C := \{z \in \mathcal{Z} : \eta_1(x_1, q_1) \leq 0, \eta_2(x_2, q_2) \leq 0\} \quad (5)$$

and the jump set is given by

$$D = \{z \in C : \eta_1(x_1, q_1) = 0\} \cup \{z \in C : \eta_2(x_2, q_2) = 0\} \quad (6)$$

To define the jump map, first note that at jumps, the continuous states x_1 and x_2 do not change. Then, we conveniently define

$$g_1(z) := \begin{bmatrix} x_1 \\ x_2 \\ 1 - q_1 \\ q_2 \end{bmatrix}, \quad g_2(z) := \begin{bmatrix} x_1 \\ x_2 \\ q_1 \\ 1 - q_2 \end{bmatrix},$$

so that the jump map G is given by

$$G(z) := \begin{cases} g_1(z) & \text{if } \eta_1(x_1, q_1) = 0, \eta_2(x_2, q_2) < 0 \\ g_2(z) & \text{if } \eta_1(x_1, q_1) < 0, \eta_2(x_2, q_2) = 0 \\ \{g_1(z), g_2(z)\} & \text{if } \eta_1(x_1, q_1) = 0, \eta_2(x_2, q_2) = 0. \end{cases} \quad (7)$$

The above definitions determine a hybrid system for (3), which is given by

$$\mathcal{H} : z \in \mathcal{Z} \begin{cases} \dot{z} = F(z) = \begin{bmatrix} k_1(1 - q_2) - \gamma_1 x_1 \\ k_2 q_1 - \gamma_2 x_2 \\ 0 \\ 0 \end{bmatrix} & z \in C \\ z^+ \in G(z) & z \in D, \end{cases} \quad (8)$$

where C is in (5), G is in (7), and D is in (6). Its parameters are given by the positive constants $k_1, k_2, \gamma_1, \gamma_2, \theta_1, \theta_2, h_1, h_2$, which satisfy $\theta_1 + h_1 < \theta_1^{\max}$, $\theta_2 + h_2 < \theta_2^{\max}$, $\theta_1 - h_1 > 0, \theta_2 - h_2 > 0$. Figure 3 depicts a hybrid automaton representation of this system when sequentially transitioning between $(q_1, q_2) = (0, 0), (1, 0), (1, 1), (0, 1)$.

Lemma 2.4 *The data (C, F, D, G) satisfies the following conditions:*

(A1) *The sets C and D are closed.*

(A2) *The map $z \mapsto F(z)$ is continuous on C .*

(A3) *The set-valued mapping $z \mapsto G(z)$ is outer semicontinuous² relative to \mathbb{R}^4 and locally bounded, and, for all $z \in D$, $G(z)$ is nonempty.*

Proof: Properties (A1) and (A2) are obvious. Property (A3) holds since the graph of G , which is given by $\{(x, y) : y \in G(x)\}$, is closed. \square

²A set-valued mapping $G : S \rightrightarrows \mathbb{R}^n$ with $S \subset \mathbb{R}^n$ is outer semicontinuous relative to S if for any $z \in S$ and any sequence $\{z_i\}_{i=1}^{\infty}$ with $z_i \in S$, $\lim_{i \rightarrow \infty} z_i = z$, and any sequence $\{w_i\}_{i=1}^{\infty}$ with $w_i \in G(z_i)$ and $\lim_{i \rightarrow \infty} w_i = w$ we have $w \in G(z)$.

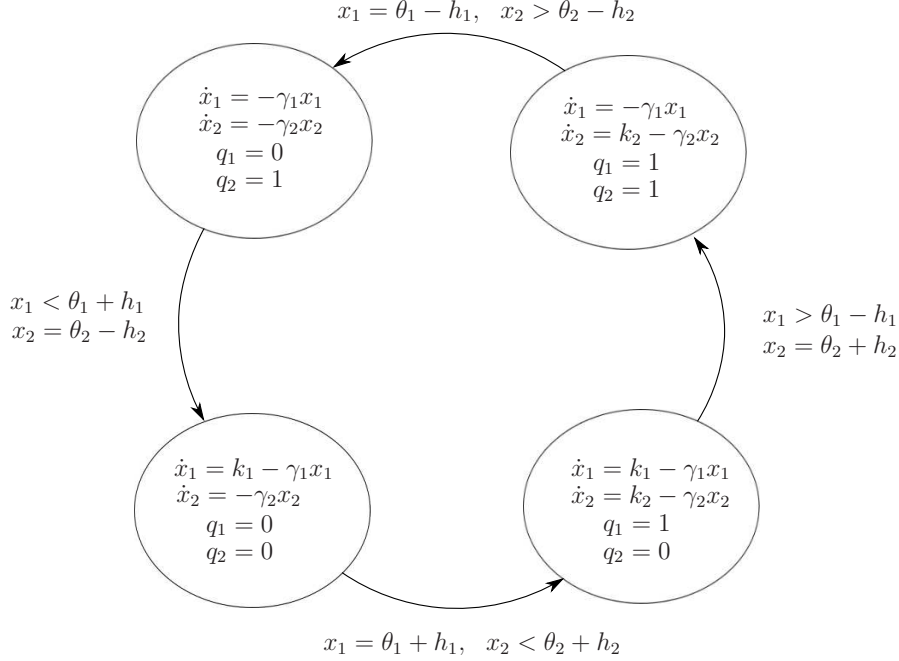


Figure 3: A hybrid automaton representation of the two-gene genetic regulatory network for sequential transitions of (q_1, q_2) .

3 Dynamical Properties of the Two-Gene Hybrid System Model

3.1 Existence of solutions

Proposition 3.1 *From every point in $C \cup D$, there exists a nontrivial solution for the hybrid system \mathcal{H} in (8). Furthermore, every maximal solution is complete and the projection of its hybrid time domain on $\mathbb{R}_{\geq 0}$ is unbounded, i.e., every solution is not Zeno.*

The proof of this result uses the conditions for the existence of solutions to \mathcal{H} in [18] for general hybrid systems. More precisely, consider the hybrid system \mathcal{H} and let $z(0, 0) \in C \cup D$. If $z(0, 0) \in D$ or

(VC) there exists a neighborhood U of $z(0, 0)$ such that³ for every $z \in U \cap C$,

$$F(z) \cap T_C(z) \neq \emptyset,$$

then there exists a nontrivial solution to \mathcal{H} from $z(0, 0)$. If (VC) holds for every $z(0, 0) \in C \setminus D$, then there exists a nontrivial solution to \mathcal{H} from every initial point in $C \cup D$, and every maximal solution z satisfies exactly one of the following conditions:

³ $T_C(z)$ denotes the tangent cone of C at z , i.e., it is the set of all v for which there exists a sequence of real numbers $\alpha_i \searrow 0$ and a sequence $v_i \rightarrow v$ such that for every $i = 1, 2, \dots$, $z + \alpha_i v_i \in C$.

1. z is complete;
2. $\text{dom } z$ is bounded and the last interval is of the form $[t_J, t_{J+1})$, where $J = \sup_{(t,j) \in \text{dom } z} j$ has nonempty interior and $t \mapsto \phi(t, J)$ is a maximal solution to $\dot{z} = F(z)$, in fact $\lim_{t \rightarrow T} |z(t, J)| = \infty$, where $T = \sup_{(t,j) \in \text{dom } z} t$;
3. $z(T, J) \notin C \cup D$, where $(T, J) = \sup \text{dom } z$.

Furthermore, if $G(D) \subset C \cup D$, then 3) above does not occur.

The proof of Proposition 3.1 uses these conditions and is given in A.2.

3.2 Characterization of equilibria

We compute the set of isolated equilibrium points z^* as well as (nonisolated, dense) sets of equilibria for the hybrid system \mathcal{H} in (8). For general hybrid systems, isolated equilibrium points are points that are an isolated equilibrium point of $\dot{z} \in F(z), z \in C$ or of $z^+ \in G(z), z \in D$. On the other hand, an equilibrium set (not necessarily an isolated equilibrium point) for a hybrid system \mathcal{H} is defined as a set that is (strongly) forward invariant.

Definition 3.2 (Equilibrium set) *A set $S \subset C \cup D$ is an equilibrium set of \mathcal{H} if for every initial condition $z(0, 0) \in S$, every solution z to \mathcal{H} satisfies $z(t, j) \in S$ for all $(t, j) \in S$.*

The following results determine the equilibria of (8) for a range of parameters of the system.

Proposition 3.3 *The equilibria of the hybrid system \mathcal{H} in (8) is given in Table 1 in terms of the positive constants $k_1, k_2, \gamma_1, \gamma_2, \theta_1, \theta_1^{\max}, \theta_2, \theta_2^{\max}, h_1$, and h_2 satisfying the conditions therein. The set $S \subset C \cup D$ in case 5 is an equilibrium set and is given by*

$$S = \bigcup_{i=1}^4 S_i, \quad (9)$$

where⁴

$$\begin{aligned} S_1 &:= \left\{ x \in \mathbb{R}^2 : x = \begin{bmatrix} \frac{k_1}{\gamma_1} - \left(\frac{k_1}{\gamma_1} - p_0(1) \right) \exp(-\gamma_1 s) \\ p_0(2) \exp(-\gamma_2 s) \end{bmatrix}, s \in [0, t'_1] \right\} \times \{(0, 0)\} \\ S_2 &:= \left\{ x \in \mathbb{R}^2 : x = \begin{bmatrix} \frac{k_1}{\gamma_1} - \left(\frac{k_1}{\gamma_1} - p_1(1) \right) \exp(-\gamma_1 s) \\ \frac{k_2}{\gamma_2} - \left(\frac{k_2}{\gamma_2} - p_1(2) \right) \exp(-\gamma_2 s) \end{bmatrix}, s \in [0, t'_2] \right\} \times \{(1, 0)\} \\ S_3 &:= \left\{ x \in \mathbb{R}^2 : x = \begin{bmatrix} p_2(1) \exp(-\gamma_1 s) \\ \frac{k_2}{\gamma_2} - \left(\frac{k_2}{\gamma_2} - p_2(2) \right) \exp(-\gamma_2 s) \end{bmatrix}, s \in [0, t'_3] \right\} \times \{(1, 1)\} \\ S_4 &:= \left\{ x \in \mathbb{R}^2 : x = \begin{bmatrix} p_3(1) \exp(-\gamma_1 s) \\ p_3(2) \exp(-\gamma_2 s) \end{bmatrix}, s \in [0, t'_4] \right\} \times \{(0, 1)\} \end{aligned}$$

⁴ $p_i(j)$ is the j -th component of p_i .

and $p_0, p_1, p_2, p_3 \in \mathbb{R}^2$ are the vertices of the set S (see Figure 4), where

$$t'_1 = \ln \left[\frac{\frac{k_1}{\gamma_1} - p_0(1)}{\frac{k_1}{\gamma_1} - (\theta_1 + h_1)} \right]^{\frac{1}{\gamma_1}}, t'_2 = \ln \left[\frac{\frac{k_2}{\gamma_2} - p_1(2)}{\frac{k_2}{\gamma_2} - (\theta_2 + h_2)} \right]^{\frac{1}{\gamma_2}},$$

$$t'_3 = \ln \left[\frac{p_2(1)}{\theta_1 - h_1} \right]^{\frac{1}{\gamma_1}}, t'_4 = \ln \left[\frac{p_3(2)}{\theta_2 - h_2} \right]^{\frac{1}{\gamma_2}},$$

and

$$p_0 = \begin{bmatrix} (\theta_1 - h_1) \left(\frac{\theta_2 - h_2}{p_3(2)} \right)^{\frac{\gamma_1}{\gamma_2}} \\ \theta_2 - h_2 \end{bmatrix}, \quad (10)$$

$$p_1 = \begin{bmatrix} \theta_1 + h_1 \\ (\theta_2 - h_2) \left(\frac{\frac{k_1}{\gamma_1} - (\theta_1 + h_1)}{\frac{k_1}{\gamma_1} - p_0(1)} \right)^{\frac{\gamma_2}{\gamma_1}} \end{bmatrix}, \quad (11)$$

$$p_2 = \begin{bmatrix} \frac{k_1}{\gamma_1} - \left(\frac{k_1}{\gamma_1} - (\theta_1 + h_1) \right) \left(\frac{\frac{k_2}{\gamma_2} - (\theta_2 + h_2)}{\frac{k_2}{\gamma_2} - p_1(2)} \right)^{\frac{\gamma_1}{\gamma_2}} \\ \theta_2 + h_2 \end{bmatrix}, \quad (12)$$

$$p_3 = \begin{bmatrix} \theta_1 - h_1 \\ \frac{k_2}{\gamma_2} - \left(\frac{k_2}{\gamma_2} - (\theta_2 + h_2) \right) \left(\frac{\theta_1 - h_1}{p_2(1)} \right)^{\frac{\gamma_2}{\gamma_1}} \end{bmatrix}. \quad (13)$$

Moreover, the period of the limit cycle is given by

$$T = t'_1 + t'_2 + t'_3 + t'_4. \quad (14)$$

The following result provides a more constructive characterization of S .

Corollary 3.4 *Under the conditions of Proposition 3.3, if furthermore, $\gamma_1 = \gamma_2 = \gamma$, then*

$$p_0(1) = \frac{-d_6 + d_8 + d_7 - d_5 - d_4 - d_3 + d_2}{d_1}, \quad (15)$$

where

$$d_1 = 2h_1k_2^2\gamma + h_2k_1k_2\gamma + k_1k_2\gamma\theta_2 - 2h_1h_2k_2\gamma^2 - 2h_1k_2\gamma^2\theta_2$$

$$d_2 = k_1k_2\gamma\theta_1\theta_2, \quad d_3 = h_2k_1k_2\gamma\theta_1, \quad d_4 = h_1k_1k_2\gamma\theta_2,$$

$$d_5 = h_1h_2k_1k_2\gamma, \quad d_7 = h_2k_1^2k_2, \quad d_8 = h_1k_1k_2^2$$

Table 1: Equilibria of the hybrid system (8).

	Conditions on constants	Equilibria
1	$\theta_1 + h_1 < \frac{k_1}{\gamma_1} < \theta_1^{\max}$ $0 < \frac{k_2}{\gamma_2} < \theta_2 + h_2$	$z_1^* := \left[\frac{k_1}{\gamma_1} \quad \frac{k_2}{\gamma_2} \quad 1 \quad 0 \right]^\top$
2	$0 < \frac{k_1}{\gamma_1} < \theta_1 - h_1$	$z_2^* := \left[\frac{k_1}{\gamma_1} \quad 0 \quad 0 \quad 0 \right]^\top$
3	$\theta_1 - h_1 < \frac{k_1}{\gamma_1} < \theta_1 + h_1$ $0 < \frac{k_2}{\gamma_2} < \theta_2 + h_2$	z_1^* or z_2^*
4	$\theta_1 - h_1 < \frac{k_1}{\gamma_1} < \theta_1 + h_1$ $\theta_2 + h_2 < \frac{k_2}{\gamma_2} < \theta_2^{\max}$	z_2^*
5	$\theta_1 + h_1 < \frac{k_1}{\gamma_1} < \theta_1^{\max}$ $\theta_2 + h_2 < \frac{k_2}{\gamma_2} < \theta_2^{\max}$	equilibrium set S defined in (9)

$$\begin{aligned}
d_6 = & k_1^{\frac{1}{2}} k_2^{\frac{1}{2}} (h_1 k_2 + h_2 k_1 - 2h_1 h_2 \gamma)^{\frac{1}{2}} \\
& (2h_1^2 h_2^2 \gamma^3 - 2h_1^2 h_2 k_2 \gamma^2 + 2h_1^2 k_2 \gamma^2 \theta_2 - 2h_1^2 \gamma^3 \theta_2^2 \\
& - 2h_1 h_2^2 k_1 \gamma^2 + d_8 - 2h_1 k_1 k_2 \gamma \theta_2 + 2h_1 k_1 \gamma^2 \theta_2^2 \\
& + 2h_2^2 k_1 \gamma^2 \theta_1 - 2h_2^2 \gamma^3 \theta_1^2 + d_7 - 2h_2 k_1 k_2 \gamma \theta_1 \\
& + 2h_2 k_2 \gamma^2 \theta_1^2 + 2k_1 k_2 \gamma \theta_1 \theta_2 - 2k_1 \gamma^2 \theta_1 \theta_2^2 \\
& - 2k_2 \gamma^2 \theta_1^2 \theta_2 + 2\gamma^3 \theta_1^2 \theta_2^2)^{\frac{1}{2}}
\end{aligned}$$

Moreover, the sets S_i are given by

$$\begin{aligned}
S_1 &= \{x \in \mathbb{R}^2 : x_2 = m_1 x_1 - m_1 p_1(1) + p_1(2), \\
&\quad p_0(1) \leq x_1 < \theta_1 + h_1, p_1(2) \leq x_2 < \theta_2 - h_2\} \times \{(0, 0)\}, \\
S_2 &= \{x \in \mathbb{R}^2 : x_2 = m_2 x_1 - m_2 p_1(1) + p_1(2), \\
&\quad \theta_1 + h_1 \leq x_1 < p_2(1), p_1(2) < x_2 \leq \theta_2 + h_2\} \times \{(1, 0)\}, \\
S_3 &= \{x \in \mathbb{R}^2 : x_2 = m_3 x_1 - m_3 p_3(1) + p_3(2), \\
&\quad \theta_1 - h_1 < x_1 \leq p_2(1), \theta_2 + h_2 < x_2 \leq p_3(2)\} \times \{(1, 1)\}, \\
S_4 &= \{x \in \mathbb{R}^2 : x_2 = m_4 x_1 - m_4 p_3(1) + p_3(2), \\
&\quad p_0(1) < x_1 \leq \theta_1 - h_1, \theta_2 - h_2 \leq x_2 < p_3(2)\} \times \{(0, 1)\},
\end{aligned}$$

where

$$\begin{aligned}
m_1 &= \frac{p_0(2) - p_1(2)}{p_0(1) - p_1(1)}, & m_2 &= \frac{p_2(2) - p_1(2)}{p_2(1) - p_1(1)}, \\
m_3 &= \frac{p_2(2) - p_3(2)}{p_2(1) - p_3(1)}, & m_4 &= \frac{p_0(2) - p_3(2)}{p_0(1) - p_3(1)}
\end{aligned} \tag{16}$$

and the points $p_0, p_1, p_2, p_3 \in \mathbb{R}^2$ are given in (10)-(13).

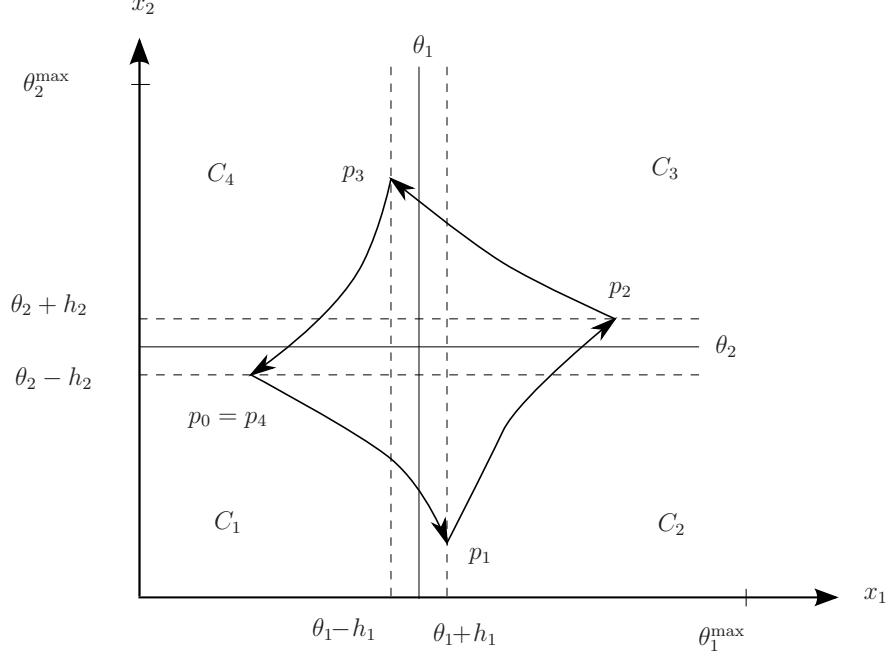


Figure 4: Set S and its vertices corresponding to case 5 of Table 1.

Proof: When $\gamma_1 = \gamma_2 = \gamma$, the definitions in (10)-(13) lead to

$$\begin{aligned}
 p_0(1) &= (\theta_1 - h_1) \left(\frac{\theta_2 - h_2}{p_3(2)} \right), \\
 p_1(2) &= (\theta_2 - h_2) \left(\frac{\frac{k_1}{\gamma} - (\theta_1 + h_1)}{\frac{k_1}{\gamma} - p_0(1)} \right) \\
 p_2(1) &= \frac{k_1}{\gamma} - \left(\frac{k_1}{\gamma} - (\theta_1 + h_1) \right) \left(\frac{\frac{k_2}{\gamma} - (\theta_2 + h_2)}{\frac{k_2}{\gamma} - p_1(2)} \right) \\
 p_3(2) &= \frac{k_2}{\gamma} - \left(\frac{k_2}{\gamma} - (\theta_2 + h_2) \right) \left(\frac{\theta_1 - h_1}{p_2(1)} \right)
 \end{aligned}$$

Letting $\lambda = p_0(1)$, we obtain

$$\begin{aligned}
 \frac{(\theta_1 - h_1)(\theta_2 - h_2)}{\lambda} &= \frac{k_2}{\gamma} - \left(\frac{k_2}{\gamma} - (\theta_2 + h_2) \right) \left(\frac{\theta_1 - h_1}{p_2(1)} \right) \\
 p_2(1) &= \frac{k_1}{\gamma} - \left(\frac{k_1}{\gamma} - (\theta_1 + h_1) \right) \left(\frac{\frac{k_2}{\gamma} - (\theta_2 + h_2)}{\frac{k_2}{\gamma} - (\theta_2 - h_2) \left(\frac{\frac{k_1}{\gamma} - (\theta_1 + h_1)}{\frac{k_1}{\gamma} - \lambda} \right)} \right)
 \end{aligned}$$

Replacing the second equation into the first one, after elementary but tedious manipulations, we obtain that $\lambda = p_0(1)$ as in (15).⁵ \square

3.3 Stability analysis

For convenience in the following analysis, we rewrite the flow set C as $C = \bigcup_{i=1}^4 C_i$ (see Figure 4), where

$$\begin{aligned} C_1 &:= \{z \in \mathcal{Z} : q_1 = 0, q_2 = 0, x_1 \leq \theta_1 + h_1, x_2 \leq \theta_2 + h_2\}, \\ C_2 &:= \{z \in \mathcal{Z} : q_1 = 1, q_2 = 0, x_1 \geq \theta_1 - h_1, x_2 \leq \theta_2 + h_2\}, \\ C_3 &:= \{z \in \mathcal{Z} : q_1 = 1, q_2 = 1, x_1 \geq \theta_1 - h_1, x_2 \geq \theta_2 - h_2\}, \\ C_4 &:= \{z \in \mathcal{Z} : q_1 = 0, q_2 = 1, x_1 \leq \theta_1 + h_1, x_2 \geq \theta_2 - h_2\}. \end{aligned}$$

3.3.1 Asymptotic stability of isolated equilibrium points

The following propositions determine the stability properties of the isolated equilibrium points in Table 1. Their proofs are in Appendix A.3 and Appendix A.4.

Proposition 3.5 *For cases 1, 2, and 4 in Table 1, the corresponding equilibrium points to \mathcal{H} in (8) are globally asymptotically stable.*

Proposition 3.6 *For case 3 in Table 1, if $z(0, 0) \in C_2$, then we have that $\lim_{t+j \rightarrow \infty} z(t, j) = z_1^*$; if $z(0, 0) \in C_1$ or $z(0, 0) \in C_4$, then $\lim_{t+j \rightarrow \infty} z(t, j) = z_2^*$. If $z(0, 0) \in C_3$, then $\lim_{t+j \rightarrow \infty} z(t, j) = z_1^*$ or z_2^* . Furthermore, z_1^* and z_2^* are stable.*

3.3.2 Stability properties of the limit cycle

Now, we determine conditions on the parameters under which the limit cycle S defined in (9) is asymptotically stable. As shown in Figure 5(b), the natural metric defined by the distance between the trajectories z of \mathcal{H} and the set S is not necessarily decreasing, even though Figure 5(a) shows that the trajectory converges to S . In fact, as depicted in the figures, the trajectory x approaches S for some time and then gets far away from it (around the corners), until a jump to a new value of q occurs.

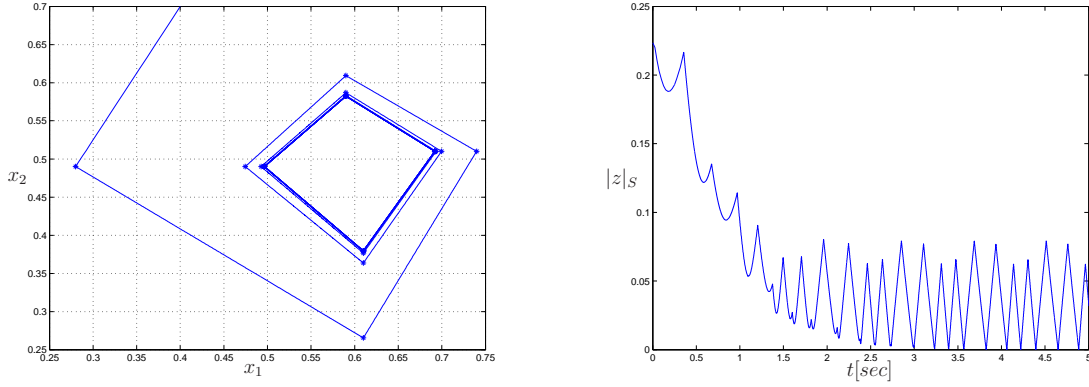
⁵When $\gamma_1 = \gamma_2 = \gamma$, the sets S_i in Proposition 3.3 reduce to straight lines. In fact, define the new coordinates

$$e := x - \begin{bmatrix} \frac{k_1(1-q_2)}{\gamma_1} \\ \frac{k_2 q_1}{\gamma_2} \end{bmatrix}. \quad (17)$$

The continuous dynamics of e are given by

$$\dot{e} = \dot{x} = \begin{bmatrix} k_1(1-q_2) - \gamma_1 x_1 \\ k_2 q_1 - \gamma_2 x_2 \end{bmatrix} = -\gamma e, \quad (18)$$

which implies that the trajectories on the plane are straight lines.



(a) Trajectory x on the plane converging to S . (b) Distance between trajectory x and the set S , denoted $|z|_S$.

Figure 5: Trajectory z of \mathcal{H} on the plane and distance between it and the set S with $\theta_1 = 0.6$, $\theta_2 = 0.5$, $\gamma_1 = 1$, $\gamma_2 = 1$, $k_1 = 1$, $k_2 = 1$, $h_1 = 0.01$, $h_2 = 0.01$, $x_1(0, 0) = 0.4$, $x_2(0, 0) = 0.4$, $q_1(0, 0) = 0$, and $q_2(0, 0) = 0$.

To overcome this issue, we augment the hybrid system \mathcal{H} with a state $\zeta \in \mathbb{R}^2$ and with continuous dynamics governed by a flow map given by a copy of the one for x , that is,

$$\dot{\zeta} = \begin{bmatrix} k_1(1 - q_2) - \gamma_1 \zeta_1 \\ k_2 q_1 - \gamma_2 \zeta_2 \end{bmatrix}.$$

The discrete dynamics of ζ are chosen so that jumps occur when jumps of \mathcal{H} occur and, at such jumps, ζ is updated via the difference inclusion

$$\zeta^+ \in \tilde{G}(x, q, \zeta).$$

To define the jump map \tilde{G} , consider the case $\gamma_1 = \gamma_2$ and, using Corollary 3.4, we extend to \mathbb{R}^2 the set of points S_i , $i \in \{1, 2, 3, 4\}$, that is, we define the (unbounded) set

$$\tilde{S} = \bigcup_{i=1}^4 \tilde{S}_i, \quad (19)$$

where

$$\begin{aligned} \tilde{S}_1 &= \{x \in \mathbb{R}^2 : x_2 = m_1 x_1 - m_1 p_1(1) + p_1(2)\} \times \{(0, 0)\}, \\ \tilde{S}_2 &= \{x \in \mathbb{R}^2 : x_2 = m_2 x_1 - m_2 p_1(1) + p_1(2)\} \times \{(1, 0)\}, \\ \tilde{S}_3 &= \{x \in \mathbb{R}^2 : x_2 = m_3 x_1 - m_3 p_3(1) + p_3(2)\} \times \{(1, 1)\}, \\ \tilde{S}_4 &= \{x \in \mathbb{R}^2 : x_2 = m_4 x_1 - m_4 p_3(1) + p_3(2)\} \times \{(0, 1)\}. \end{aligned}$$

During flows, the set \tilde{S} is forward invariant for the state component ζ (both during flows and jumps) along the dynamics of q governed by \mathcal{H} . This is the reason we restrict ζ to belong to \tilde{S} for the current value of q . Then, due to the stability properties of the error system with state $\zeta - x$, the distance between x and ζ strictly decreases during flows. With this useful property of the trajectories while flowing, at jumps due to \mathcal{H} , which occur when

$(x(t, j), q(t, j)) \in D$ and map $q(t, j)$ to $q(t, j + 1)$ (following the definition of G in (7)), the jump map \tilde{G} is constructed to map the state ζ to satisfy $(\zeta(t, j + 1), q(t, j + 1)) \in \tilde{S}$ such that, if $(\zeta(t, j), q(t, j)) \in \tilde{S}_{q(t, j)}$ before the jump, then $(\zeta(t, j + 1), q(t, j + 1)) \in \tilde{S}_{q(t, j + 1)}$ and with the property that

$$\text{dist}(x(t, j + 1), \zeta(t, j + 1)) \leq \text{dist}(x(t, j), \zeta(t, j))$$

where dist is the Euclidean distance between two points in \mathbb{R}^2 . In this way, the new value of ζ at jumps can be determined for each $x \in \mathbb{R}^2$ from the set

$$\tilde{g}(x, q, \zeta) := \left\{ \zeta' : \text{dist}(x, \zeta') \leq \text{dist}(x, \zeta), (\zeta', q') \in \tilde{S}_{q'}, (x, q') \in G(x, q) \right\}$$

(when it is not empty). Since the distance between x and ζ decreases during flows, asymptotic stability of \tilde{S} can be established when $\tilde{G}(x, q, \zeta)$ is nonempty since this guarantees that the distance between x and ζ is nonincreasing. The following result imposes conditions on the parameters guaranteeing that \tilde{G} is nonempty and, furthermore, extends the attractivity property to the set S .

Theorem 3.7 *For positive constants $k_1, k_2, \gamma_1, \gamma_2, \theta_1, \theta_1^{\max}, \theta_2, \theta_2^{\max}, h_1,$ and h_2 such that*

$$\gamma_1 = \gamma_2 = \gamma, \quad |m_1| \leq \min\{|m_2|, |m_4|\}, \quad |m_3| \leq \min\{|m_2|, |m_4|\}, \quad (20)$$

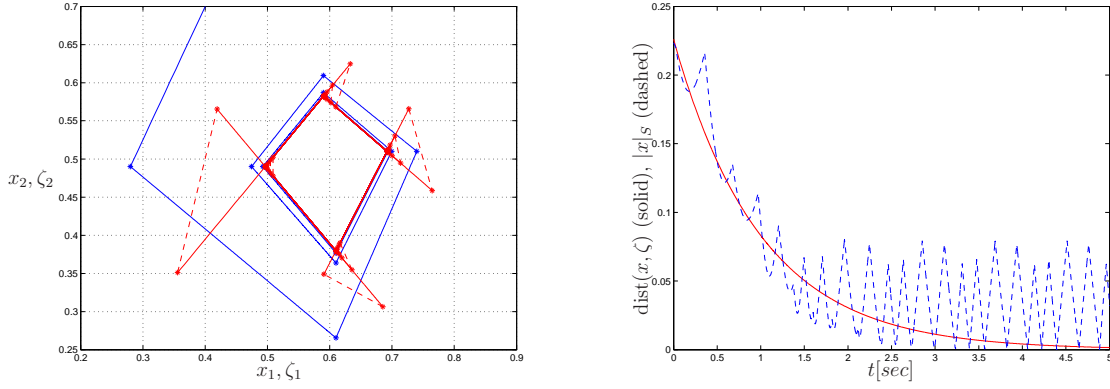
where, for each $i \in \{1, 2, 3, 4\}$, m_i are given in (16), the following holds:

1. The set \tilde{S} is globally asymptotically stable for \mathcal{H} . In particular, each maximal solution to \mathcal{H} satisfies

$$d((x(t, j), q(t, j)), \tilde{S}) \leq \exp(-\gamma t) d((x(0, 0), q(0, 0)), \tilde{S}) \quad (21)$$

for all $(t, j) \in \text{dom}(x, q)$, where $d((x, q), \tilde{S}) = \min_{(\zeta, q) \in \tilde{S}} |x - \zeta|$.

2. The set S in case 5 of Table 1 is globally attractive for \mathcal{H} , i.e., every solution to \mathcal{H} converges to S .



(a) Trajectories x and ζ on the plane.

(b) Distance between trajectory x and ζ (solid), and distance between x and S (dashed).

Figure 6: Trajectories x and ζ on the plane, and distance between x and ζ compared to distance between x and the set S (dashed) with the same parameters and initial conditions as in Figure 5.

Figure 6 shows trajectories x and ζ as well as the distance between them obtained from the hybrid system augmented with the state ζ . As Figure 6(b) indicates, this distance (solid) decreases to zero while, as pointed out earlier, the natural distance between x and S (dashed) does not. The extended version of the hybrid system \mathcal{H} in (8) can be written as

$$\tilde{\mathcal{H}} : (x, q, \zeta) \in \mathcal{Z} \times \mathbb{R}_{\geq 0}^2 \left\{ \begin{array}{l} \begin{array}{l} \begin{bmatrix} \dot{x}_1 \\ \dot{x}_2 \\ \dot{q}_1 \\ \dot{q}_2 \\ \dot{\zeta}_1 \\ \dot{\zeta}_2 \end{bmatrix} = \begin{bmatrix} k_1(1 - q_2) - \gamma_1 x_1 \\ k_2 q_1 - \gamma_2 x_2 \\ 0 \\ 0 \\ k_1(1 - q_2) - \gamma_1 \zeta_1 \\ k_2 q_1 - \gamma_2 \zeta_2 \end{bmatrix} =: \tilde{F}(x, q, \zeta) \\ (x, q) \in C, (\zeta, q) \in \tilde{S}, \\ \begin{bmatrix} z^+ \\ \zeta^+ \end{bmatrix} \in \begin{bmatrix} G(z) \\ \tilde{G}(x, q, \zeta) \end{bmatrix} =: \tilde{G}(x, q, \zeta) \\ (x, q) \in D, (\zeta, q) \in \tilde{S}. \end{array} \right. \quad (22)$$

We are now ready to prove Theorem 3.7.

Proof: (of Theorem 3.7) First, we show that \tilde{G} is nonempty for each (x, q, ζ) such that $(x, q) \in D$ and $(\zeta, q) \in \tilde{S}$. For each $(x, q) \in D$, the minimum possible value for $\text{dist}(x, \zeta)$ with $(\zeta, q) \in \tilde{S}$ is given by the minimum distance between x and the projection on \mathbb{R}^2 of \tilde{S} for the chosen q . There are four possible cases for this distance (one per possible value of q) and each distance can be computed as the minimum distance between the point x and the line defined by \tilde{S} for the chosen q . For jumps from $q = (0, 1)$ to $q = (0, 0)$, in which case $x_1 \in [0, p_0(1)]$, $x_2 = \theta_2 - h_2$, the minimum distance is

$$\frac{|m_4| |x_1 - p_0(1)|}{\sqrt{m_4^2 + 1}} \quad (23)$$

Similarly, the minimum distance from x to the line defined by \tilde{S} for $q = (0, 0)$, which is the distance between (x, q) and \tilde{S} after the jump, is given by

$$\frac{|m_1||x_1 - p_0(1)|}{\sqrt{m_1^2 + 1}}. \quad (24)$$

Then, imposing that (24) is no larger than (23) guarantees that, in the worst case, $\text{dist}(x, \zeta') \leq \text{dist}(x, \zeta)$. Then, we require

$$\frac{|m_1||x_1 - p_0(1)|}{\sqrt{m_1^2 + 1}} \leq \frac{|m_4||x_1 - p_0(1)|}{\sqrt{m_4^2 + 1}} \iff |m_1| \leq |m_4|. \quad (25)$$

Proceeding in this way, for jumps from $q = (0, 0)$ to $q = (1, 0)$, from $q = (1, 0)$ to $q = (1, 1)$, and from $q = (1, 1)$ to $q = (0, 1)$ we require

$$|m_1| \leq |m_2|, \quad |m_3| \leq |m_2|, \quad |m_3| \leq |m_4|, \quad (26)$$

respectively. Under these conditions, which can be rewritten as in (20), \tilde{G} is nonempty.

For each $(x, q, \zeta) \in \mathbb{R}^2 \times \{0, 1\}^2 \times \mathbb{R}^2$, let

$$V(x, q, \zeta) = \text{dist}(x, \zeta)^2$$

and note that V is positive definite with respect to the closed set

$$\mathcal{A} := \left\{ (x, q, \zeta) : x = \zeta, (x, q) \in C \cup D, (\zeta, q) \in \tilde{S} \right\}. \quad (27)$$

For each $(x, q) \in C$ and $(\zeta, q) \in \tilde{S}$, we obtain

$$\begin{aligned} \langle \nabla V(x, q, \zeta), \tilde{F}(x, q, \zeta) \rangle &= -2(\gamma_1(x_1 - \zeta_1)^2 + \gamma_2(x_2 - \zeta_2)^2) \\ &= -2\gamma V(x, q, \zeta), \end{aligned} \quad (28)$$

where we have used the condition $\gamma_1 = \gamma_2 = \gamma$. For each $(x, q) \in D$ and $(\zeta, q) \in \tilde{S}$, we have

$$\begin{aligned} \max_{\xi \in \tilde{G}(x, q, \zeta)} V(\xi) - V(x, q, \zeta) &= \max_{(x, \xi_2) \in G(x, q), (\xi_3, \xi_2) \in \tilde{G}(x, q, \zeta)} \text{dist}(x, \xi_3)^2 - \text{dist}(x, \zeta)^2 \\ &\leq 0 \end{aligned} \quad (29)$$

since, by definition of \tilde{G} , we have that any possible value of ξ_3 obtained from \tilde{G} is such that $\text{dist}(x, \xi_3)^2 \leq \text{dist}(x, \zeta)^2$. Then, since every maximal solution to \mathcal{H} (and, hence, to $\tilde{\mathcal{H}}$) is complete and has a hybrid time domain unbounded in the t direction, [20, Proposition 3.29] implies that \mathcal{A} is globally asymptotically stable.⁶ In fact, combining (28) and (29), and simple integration, we get that every solution (x, q, ζ) to $\tilde{\mathcal{H}}$ satisfies

$$\text{dist}(x(t, j), \zeta(t, j)) \leq \exp(-\gamma t) \text{dist}(x(0, 0), \zeta(0, 0)) \quad (30)$$

for all $(t, j) \in \text{dom}(x, q, \zeta)$.

⁶The same result can be obtained using the invariance principle for hybrid systems in [21].

Now, we relate the asymptotic stability property above to \tilde{S} . The bound (30) holds for any $\zeta(0, 0)$ such that $(\zeta(0, 0), q(0, 0)) \in \tilde{S}$, in particular, when $\zeta(0, 0)$ is such that⁷ $\text{dist}(x(0, 0), \zeta(0, 0)) = d((x(0, 0), q(0, 0)), \tilde{S})$. Moreover, note that since $(\zeta(t, j), q(t, j)) \in \tilde{S}$ for all $(t, j) \in \text{dom}(x, q, \zeta)$, we have

$$d((x(t, j), q(t, j)), \tilde{S}) \leq \text{dist}(x(t, j), \zeta(t, j)) \quad (31)$$

for all $(t, j) \in \text{dom}(x, q, \zeta)$. Then, from (30) and the above arguments, we obtain

$$d((x(t, j), q(t, j)), \tilde{S}) \leq \exp(-\gamma t) d((x(0, 0), q(0, 0)), \tilde{S}) \quad (32)$$

for all $(t, j) \in \text{dom}(x, q, \zeta)$.

To show that the components (x, q) of the solutions to $\tilde{\mathcal{H}}$ converge to S , we proceed by contradiction and suppose that there exists a maximal solution to $\tilde{\mathcal{H}}$ with components (x, q) with ω -limit set $\Omega(x, q)$ such that $\Omega(x, q) \cap (\tilde{S} \setminus S) \neq \emptyset$. Let $z^\circ \in \Omega(x, q) \cap (\tilde{S} \setminus S) \neq \emptyset$. By the properties of the ω -limit set of complete solutions to hybrid systems (see [21, Definition 3.2 and Lemma 3.3]), there exists at least one solution starting from z° , which is impossible since points in $\tilde{S} \setminus S$ are not in $C \cup D$ and $\tilde{\mathcal{H}}$ satisfies the hybrid basic conditions. Then, $\Omega(x, q)$ cannot contain points that are not in S , which implies that $\Omega(x, q) \subset S$. Convergence of components (x, q) of the solutions to $\tilde{\mathcal{H}}$ to S follows by the very definition of ω -limit set of a solution. □

3.4 Robustness properties

When the system \mathcal{H} in (8) is restricted to a compact set of the initial conditions for the state component x , the asymptotic stability of the set \tilde{S} guaranteed in Theorem 3.7 is robust to small perturbations. We define this set of initial conditions as the compact box in $\mathbb{R}_{\geq 0}^2$ as

$$K := [0, x_1^{\max}] \times [0, x_2^{\max}]$$

with positive constants x_1^{\max} and x_2^{\max} such that $S \subset K \times \{0, 1\}^2$. We consider perturbations on the state and on the continuous dynamics of the system. The signal $d_1 : \mathbb{R}_{\geq 0} \rightarrow \delta_1 \mathbb{B} \subset \mathbb{R}^2$ defines the perturbation on the state and the signal $d_2 : \mathbb{R}_{\geq 0} \rightarrow \delta_2 \mathbb{B} \subset \mathbb{R}^2$ defines the perturbation on the flow of x , where $\delta_1, \delta_2 > 0$. In this way, the perturbed hybrid system is given by

$$\mathcal{H}_\delta : z \in \mathcal{Z} \begin{cases} \dot{z} = \begin{bmatrix} k_1(1 - q_2) - \gamma_1(x_1 + d_{11}(t)) + d_2(t) \\ k_2 q_1 - \gamma_2(x_2 + d_{12}(t)) + d_2(t) \\ 0 \\ 0 \end{bmatrix} & (x + d_1(t), q) \in C \cap K \\ z^+ \in G(z) & (x + d_1(t), q) \in D \cap K, \end{cases} \quad (33)$$

where C is defined in (5), G in (7), and D in (6). The perturbation d_1 captures uncertainty in the values of the protein concentrations x while d_2 models the uncertainty in the dynamical

⁷Note that we could also pick $\zeta(0, 0)$ such that the distance to S matches.

model governing x .⁸ In particular, the latter perturbation allows for uncertainty in the parameters k_1, k_2 . For instance, if k_1 is replaced by $k_1 + k_1^\delta$ with $k_1^\delta \in \mathbb{R}$ then the continuous dynamics of x_1 along a solution (x, q) to \mathcal{H} can be rewritten as

$$\begin{aligned} \frac{d}{dt}x_1(t, j) &= (k_1 + k_1^\delta)(1 - q_2(t, j)) - \gamma_1(x_1 + d_{11}(t)) \\ &= k_1(1 - q_2(t, j)) - \gamma_1(x_1(t, j) + d_{11}(t)) + k_1^\delta(1 - q_2(t, j)), \end{aligned}$$

which leads to⁹ $d_{21}(t) = k_1^\delta(1 - q_2(t, j(t)))$. Note that since q_2 takes values from $\{0, 1\}$, then we have that $|d_2(t)| \leq \delta_2$ when $|k_1^\delta| \leq \frac{\sqrt{2}}{2}\delta_2$.

Due to \mathcal{H} satisfying conditions (A1)-(A3) in Lemma 2.4, the stability property guaranteed by Theorem 3.7 is robust to small perturbations. This property follows from the results on robustness of stability for hybrid systems in [20].

Theorem 3.8 *For each positive constants x_1^{\max} and x_2^{\max} defining $K := [0, x_1^{\max}] \times [0, x_2^{\max}]$ such that $S \subset K \times \{0, 1\}^2$ and system constants satisfying case 5 of Table 1, there exists¹⁰ $\beta \in \mathcal{KL}$ such that, for each $\varepsilon > 0$ there exists $\delta > 0$ such that for each measurable functions $d_1 : \mathbb{R}_{\geq 0} \rightarrow \delta_1\mathbb{B}$, $d_2 : \mathbb{R}_{\geq 0} \rightarrow \delta_2\mathbb{B}$ with $\delta_1, \delta_2 \in (0, \delta]$, every solution (x, q) to \mathcal{H}_δ with $(x(0, 0), q(0, 0)) \in K$ satisfies*

$$|(x(t, j), q(t, j))|_{\tilde{S} \cap K} \leq \beta(|(x(0, 0), q(0, 0))|_{\tilde{S} \cap K}, t + j) + \varepsilon \quad \forall (t, j) \in \text{dom}(x, q).$$

4 Numerical results

In this section, we simulate the hybrid system \mathcal{H} in (8) within Matlab/Simulink using the HyEQ Toolbox [22].

4.1 Isolated equilibrium points in Table 1

We perform simulations with parameters satisfying the conditions in Table 1 for which there are isolated equilibrium points.

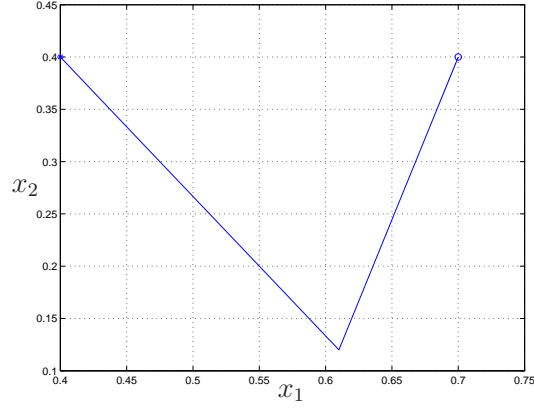
4.1.1 Case 1 of Table 1

Figure 7 illustrates that, when $\theta_1 + h_1 < \frac{k_1}{\gamma_1} < \theta_1^{\max}$, $0 < \frac{k_2}{\gamma_2} < \theta_2 + h_2$, the solution converges to $z_1^* = [\frac{k_1}{\gamma_1}, \frac{k_2}{\gamma_2}, 1, 0]^\top$. Initially, the concentration of protein A (x_1) is low, which inhibits the expression of gene b , hence the concentration of protein B (x_2) decreases and activates the expression of gene a . However, after finite time, while the concentration of protein A is above the level $\theta_1 + h_1$, which can permit the expression of gene b , the concentration of protein B increases. Finally, the concentrations of protein A and B come to the equilibrium $(\frac{k_1}{\gamma_1}, \frac{k_2}{\gamma_2})$. This confirms the result in Proposition 3.5.

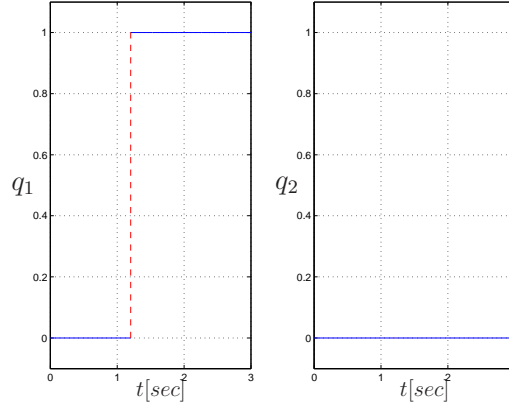
⁸Perturbations on each of the system parameters, in particular, the thresholds θ_i and hysteresis half widths h_i , can be treated similarly.

⁹For each t such that $(t, j) \in \text{dom}(x, q)$, the function $j : \mathbb{R}_{\geq 0} \rightarrow \mathbb{N}$ is given by $j(t) = j'$, where $j' = \max\{j : (t, j) \in \text{dom}(x, q)\}$.

¹⁰A function β is of class \mathcal{KL} if it is continuous, $r \mapsto \beta(r, s)$ is zero at zero and nondecreasing, and



(a) x components.



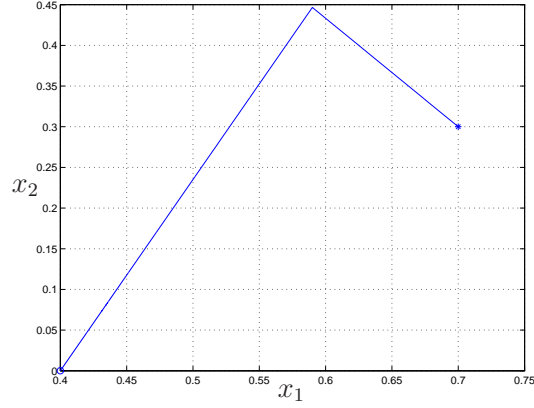
(b) q components.

Figure 7: The x and q components of a solution to \mathcal{H} in (8) converging to z_1^* . The initial condition is given by $q_1(0,0) = 0$, $q_2(0,0) = 0$, $x_1(0,0) = 0.4$, $x_2(0,0) = 0.4$. The parameters are as follows: $\theta_1 = 0.6$, $\theta_2 = 0.5$, $k_1 = 0.7$, $k_2 = 0.4$, $\gamma_1 = 1$, $\gamma_2 = 1$, $h_1 = 0.01$, $h_2 = 0.01$. The symbol $*$ denotes the initial point and \circ the point that the solution converges to (i.e., z_1^*).

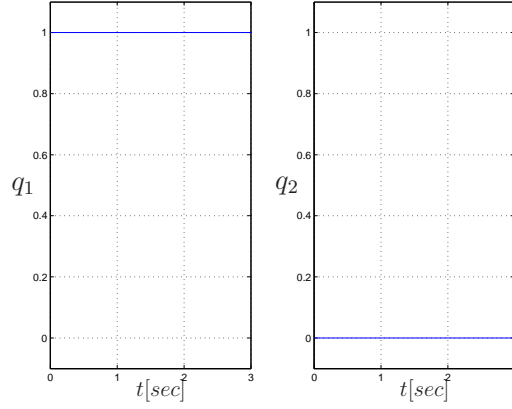
4.1.2 Case 2 of Table 1

Figure 8 shows a solution to the equilibrium point $z_2^* = [\frac{k_1}{\gamma_1}, 0, 0, 0]^T$ with $0 < \frac{k_1}{\gamma_1} < \theta_1 - h_1$. While both gene a and gene b are expressed at rate k_i , for gene a , its degradation is faster than synthesis. When the concentration of protein A (x_1) is below some level, gene b is inhibited. This confirms the result in Proposition 3.5.

$s \mapsto \beta(r, s)$ is nonincreasing and converges to zero as s goes to ∞ .



(a) x components.



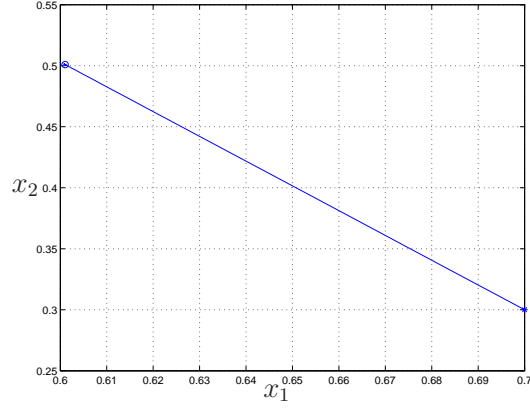
(b) q components.

Figure 8: The x and q components of a solution to \mathcal{H} in (8) converging to z_2^* . The initial condition is given by $q_1(0, 0) = 1$, $q_2(0, 0) = 0$, $x_1(0, 0) = 0.7$, $x_2(0, 0) = 0.3$. The parameters are as follows: $\theta_1 = 0.6$, $\theta_2 = 0.5$, $k_1 = 0.4$, $k_2 = 0.7$, $\gamma_1 = 1$, $\gamma_2 = 1$, $h_1 = 0.01$, $h_2 = 0.01$. The symbol $*$ denotes the initial point and \circ is the point that the solution converges to (i.e., z_2^*).

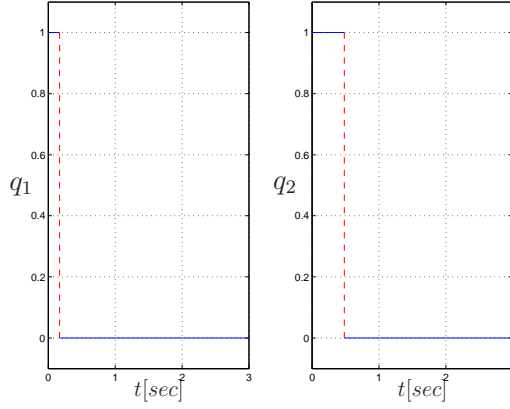
4.1.3 Case 3 of Table 1

Figure 9 indicates that, when $\theta_1 - h_1 < \frac{k_1}{\gamma_1} < \theta_1 + h_1$, $0 < \frac{k_2}{\gamma_2} < \theta_2 + h_2$ with the initial value $z(0, 0) \in C_2 := \{q_1 = 1, q_2 = 0, x_1 \geq \theta_1 - h_1, x_2 \leq \theta_2 + h_2\}$. The solution flows towards $z_1^* = [\frac{k_1}{\gamma_1}, \frac{k_2}{\gamma_2}, 1, 0]^\top$. Under these conditions, gene a and gene b are expressed at rate k_i , $i = 1, 2$, respectively. However, for gene a , its degradation is faster than its synthesis. This confirms the result in Proposition 3.6.

Figure 10 illustrates the case when $\theta_1 - h_1 \leq \frac{k_1}{\gamma_1} \leq \theta_1 + h_1$, $\frac{k_2}{\gamma_2} \leq \theta_2 + h_2$. With the initial value $z(0, 0) \notin C_2$, the solution converges to $z_2^* = [\frac{k_1}{\gamma_1}, 0, 0, 0]^\top$. With these conditions, initially, gene b is expressed at k_2 and gene a is inhibited. After finite time, as the concen-



(a) x components.



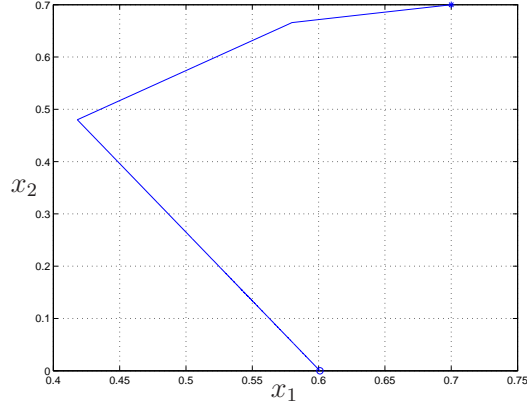
(b) q components.

Figure 9: The x and q components of a solution to \mathcal{H} in (8) converging to z_1^* . The initial conditions are given by $q_1(0,0) = 1$, $q_2(0,0) = 0$, $x_1(0,0) = 0.7$, $x_2(0,0) = 0.3$. The parameters are as follows: $\theta_1 = 0.6$, $\theta_2 = 0.5$, $k_1 = 0.601$, $k_2 = 0.501$, $\gamma_1 = 1$, $\gamma_2 = 1$, $h_1 = 0.02$, $h_2 = 0.02$. The symbol $*$ denotes the initial point and \circ is the point that the solution converges to (i.e., z_1^*).

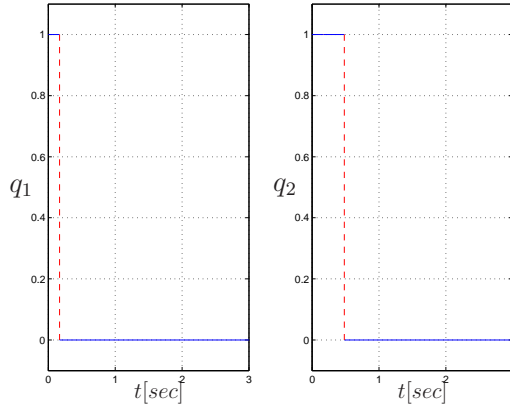
tration of protein A (x_1) is lower than $\theta_1 - h_1$, gene b becomes inhibited. Gene a is expressed at k_1 while the concentration of protein B (x_2) is below a certain level. This confirms the result in Proposition 3.6.

4.1.4 Case 4 of Table 1

Figure 11 indicates that, when $\theta_1 - h_1 < \frac{k_1}{\gamma_1} < \theta_1 + h_1$, $\theta_2 + h_2 < \frac{k_2}{\gamma_2} < \theta_2^{max}$ with the initial value $z(0,0) \in C_2 := \{q_1 = 1, q_2 = 0, x_1 \geq \theta_1 - h_1, x_2 \leq \theta_2 + h_2\}$. The solution flows towards $z_2^* = [\frac{k_1}{\gamma_1}, 0, 0, 0]^T$. Under these conditions, gene a and gene b are expressed at rate k_i , $i = 1, 2$ initially. After some time, the concentration of protein B exceeds a certain level, which triggers a jump, after which the expression of gene a is inhibited. When the



(a) x components.



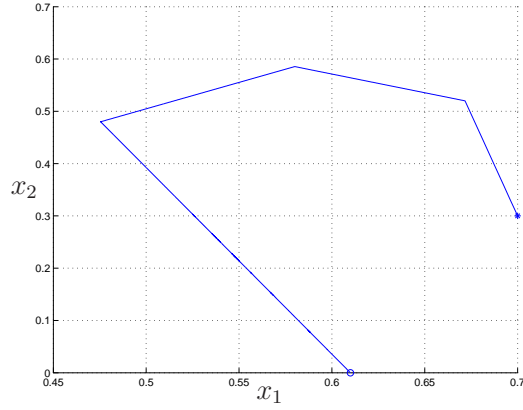
(b) q components.

Figure 10: The x and q components of a solution to \mathcal{H} in (8) converging to z_1^* . The initial conditions are given by $q_1(0,0) = 1$, $q_2(0,0) = 1$, $x_1(0,0) = 0.7$, $x_2(0,0) = 0.7$. The parameters are as follows: $\theta_1 = 0.6$, $\theta_2 = 0.5$, $k_1 = 0.601$, $k_2 = 0.501$, $\gamma_1 = 1$, $\gamma_2 = 1$, $h_1 = 0.02$, $h_2 = 0.02$. The symbol $*$ is the initial point and \circ is the point that the solution converges to (i.e., z_2^*).

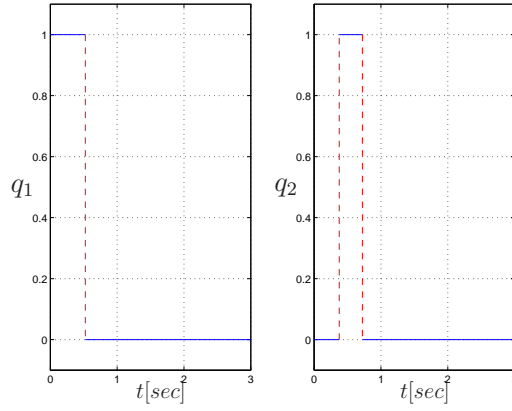
concentration of protein A decreases enough, another jump occurs, after which the expression of gene b is inhibited as well. Eventually, the concentration of protein B reaches a low enough value to trigger another jump, after which the expression of gene a is activated, and the concentrations approach a steady-state value. This simulation confirms the result in Proposition 3.6.

4.2 Equilibrium set S

When the parameters are in the region $\theta_1 + h_1 < \frac{k_1}{\gamma_1} < \theta_1^{\max}$, $\theta_2 + h_2 < \frac{k_2}{\gamma_2} < \theta_2^{\max}$, the set of points S in (9) defines the equilibria. First, we compute this set of points for particular values of $k_1, k_2, h_1, h_2, \gamma_1 = \gamma_2 = \gamma, \theta_1, \theta_2$. Let $k_1 = 1$, $k_2 = 1$, $\gamma_1 = \gamma_2 = \gamma = 1$, $\theta_1 = 0.6$, $\theta_2 = 0.5$,



(a) x components.



(b) q components.

Figure 11: The x and q components of a solution to \mathcal{H} in (8) converging to z_2^* . The initial conditions are given by $q_1(0,0) = 1$, $q_2(0,0) = 0$, $x_1(0,0) = 0.7$, $x_2(0,0) = 0.3$. The parameters are as follows: $\theta_1 = 0.6$, $\theta_2 = 0.5$, $k_1 = 0.61$, $k_2 = 1$, $\gamma_1 = 1$, $\gamma_2 = 1$, $h_1 = 0.02$, $h_2 = 0.02$. The symbol $*$ denotes the initial point and \circ is the point that the solution converges to (i.e., z_2^*).

$h_1 = 0.01$, $h_2 = 0.01$. Then, using Corollary 3.4, the point p_0 is given by $p_0(1) = 0.4966$. Then, from (10)-(13), we obtain $p_0 = \begin{bmatrix} 0.4966 \\ 0.49 \end{bmatrix}$, $p_1 = \begin{bmatrix} 0.61 \\ 0.3796 \end{bmatrix}$, $p_2 = \begin{bmatrix} 0.692 \\ 0.51 \end{bmatrix}$, $p_3 =$

$\begin{bmatrix} 0.59 \\ 0.5822 \end{bmatrix}$. With the values of p_0, p_1, p_2, p_3 , the set S in (9) is given by

$$\begin{aligned}
S_1 &= \{x : x_2 = -0.973381x_1 + 0.973381, \\
&\quad 0.4966 \leq x_1 \leq 0.61, 0.3796 \leq x_2 \leq 0.49\} \times \{(0, 0)\}, \\
S_2 &= \{x : x_2 = 1.590722x_1 - 0.590722, \\
&\quad 0.61 \leq x_1 \leq 0.692, 0.3796 \leq x_2 \leq 0.51\} \times \{(1, 0)\}, \\
S_3 &= \{x : x_2 = -0.7081296x_1 + 1, \\
&\quad 0.59 \leq x_1 \leq 0.692, 0.51 \leq x_2 \leq 0.5822\} \times \{(1, 1)\}, \\
S_4 &= \{x : x_2 = 0.9871896x_1 - 0.000238, \\
&\quad 0.4966 \leq x_1 \leq 0.59, 0.49 \leq x_2 \leq 0.5822\} \times \{(0, 1)\}.
\end{aligned}$$

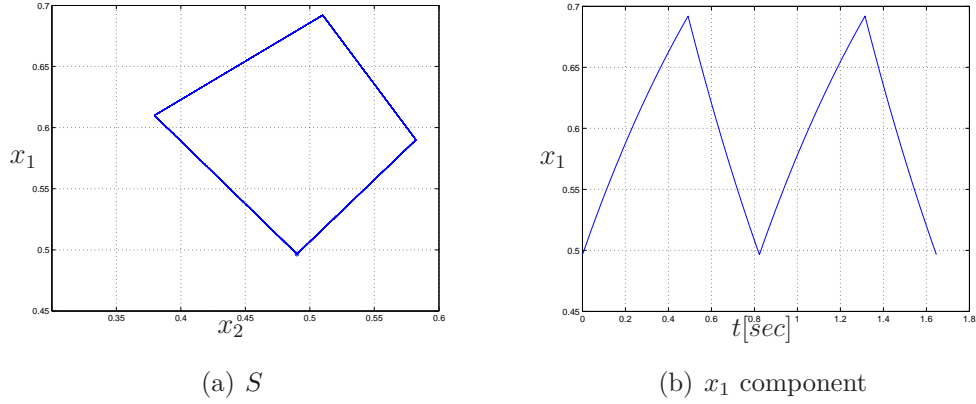
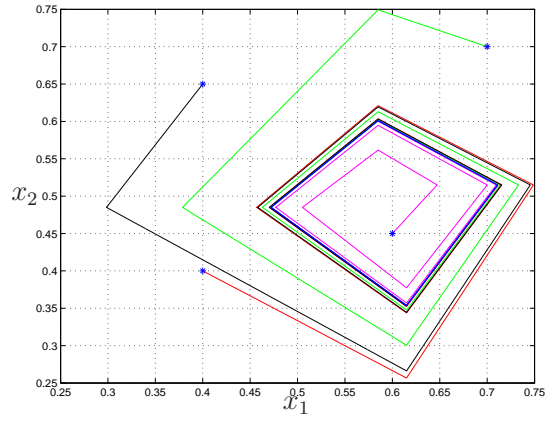
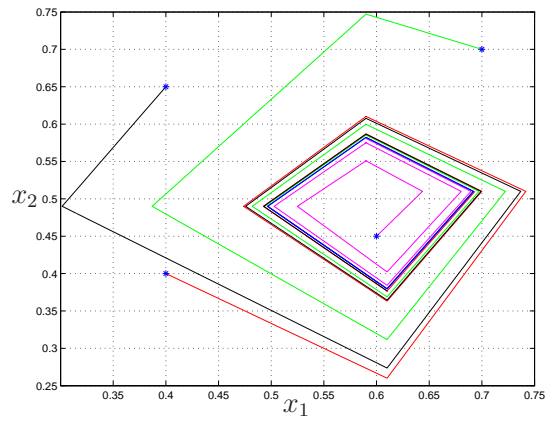


Figure 12: *Set S for parameters $k_1 = 1, k_2 = 1, \gamma_1 = 1, \gamma_2 = 1, \theta_1 = 0.6, \theta_2 = 0.5, h_1 = 0.01, h_2 = 0.01$.*

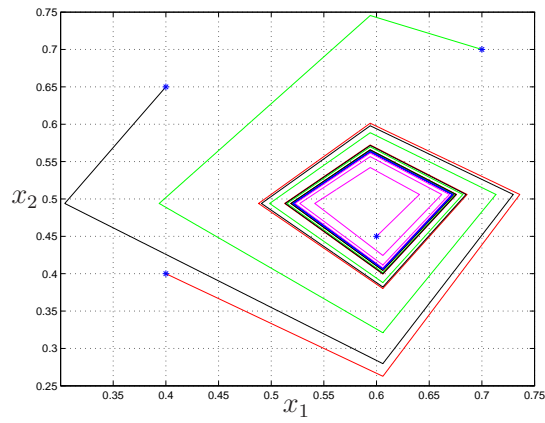
Figure 12(a) shows the set of points S projected to \mathbb{R}^2 for these parameters. For the same parameter values, the period of the limit cycle obtained from Corollary 3.4 is $T = 0.8230$ sec, where $t'_1 = 0.2552$ sec, $t'_2 = 0.2359$ sec, $t'_3 = 0.1594$ sec, $t'_4 = 0.1724$ sec. Figure 12(b) confirms this result.



(a) $h_1 = 0.015, h_2 = 0.015$



(b) $h_1 = 0.01, h_2 = 0.01$



(c) $h_1 = 0.006, h_2 = 0.006$

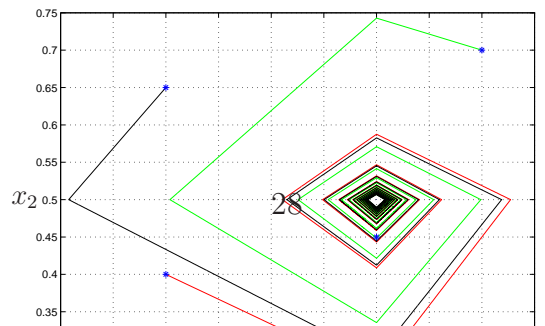
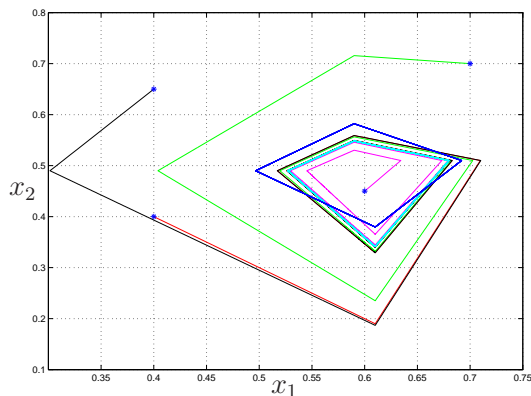
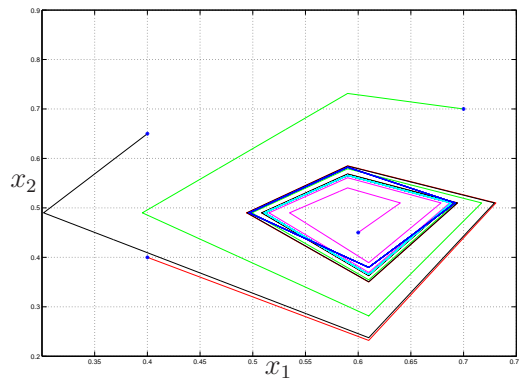


Figure 13 shows simulations with several initial conditions and common parameters $\theta_1 = 0.6, \theta_2 = 0.5, \gamma_1 = 1, \gamma_2 = 1, k_1 = 1, k_2 = 1$, but decreasing h_1, h_2 . Each solution converges to the limit cycle S . The size of the limit cycle is reduced as h_1, h_2 gets smaller. From our results we know that the size of the limit cycle depends on the value of hysteresis parameters. When the magnitude of hysteresis tends to zero, the set S approaches a point, which is given by (θ_1, θ_2) (see similar case shown in Figure 13(d).)

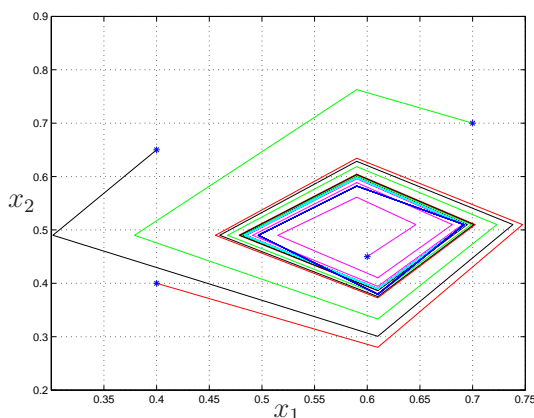
Figure 14 shows simulations with several initial conditions and common parameters $\theta_1 = 0.6, \theta_2 = 0.5, \gamma_1 = 1, \gamma_2 = 1, h_1 = 0.01, h_2 = 0.01$, but changing k_1, k_2 . Each solution converges to the limit cycle S (in cyan). The blue set of points defines the limit cycle S generated when $k_1 = k_2 = 1$. The variations of k_1 and k_2 can be considered to be perturbations as in Theorem 3.8. The simulations show that the smaller the perturbation on these constants, the closer the limit cycle becomes to the nominal one. Figure 15 shows simulations with several initial conditions and common parameters $\theta_1 = 0.6, \theta_2 = 0.5, k_1 = 1, k_2 = 1, h_1 = 0.01, h_2 = 0.01$, but now with γ_1 and γ_2 varying.



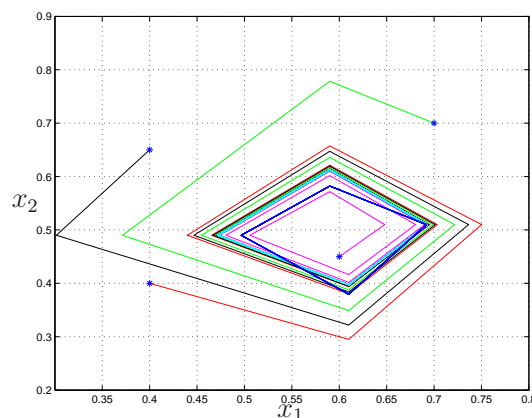
(a) $k_1 = 0.8, k_2 = 0.8$



(b) $k_1 = 0.9, k_2 = 0.9$

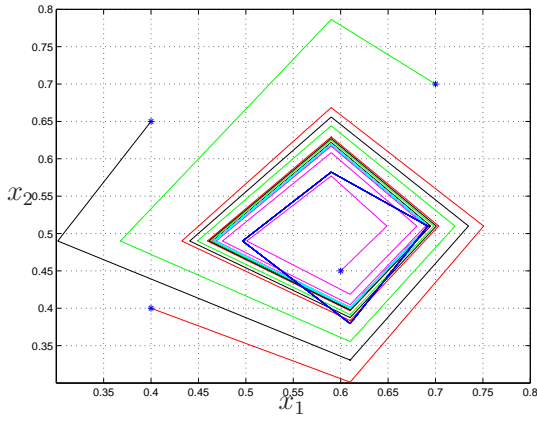


(c) $k_1 = 1.1, k_2 = 1.1$

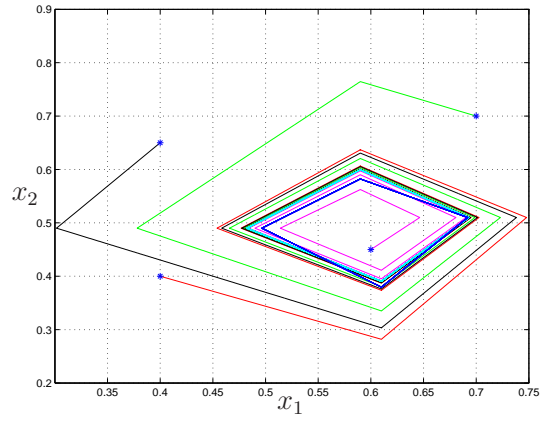


(d) $k_1 = 1.2, k_2 = 1.2$

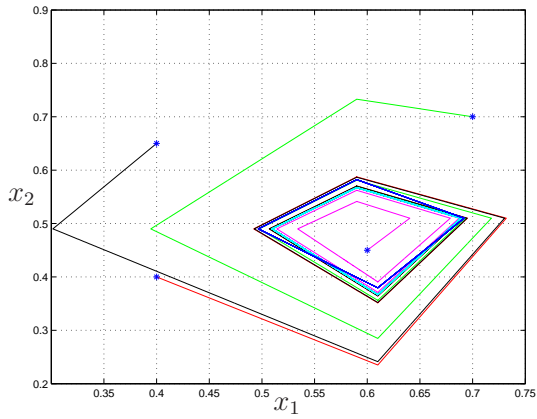
Figure 14: Solutions approaching the set S with different initial conditions of z and fixed parameters $\theta_1 = 0.6, \theta_2 = 0.5, \gamma_1 = 1, \gamma_2 = 1, h_1 = 0.01, h_2 = 0.01$.



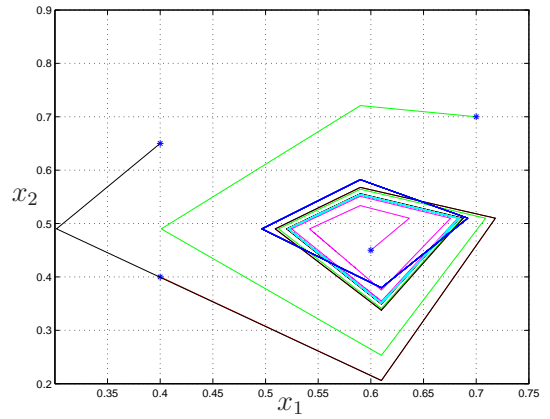
(a) $k_1 = 0.8, k_2 = 0.8$



(b) $\gamma_1 = 0.9, \gamma_2 = 0.9$



(c) $\gamma_1 = 1.1, \gamma_2 = 1.1$



(d) $\gamma_1 = 1.2, \gamma_2 = 1.2$

Figure 15: Solutions approaching the set S with different initial conditions of z and fixed parameters $\theta_1 = 0.6, \theta_2 = 0.5, k_1 = 1, k_2 = 1, h_1 = 0.01, h_2 = 0.01$.

Finally, Figure 16 shows the case when $\gamma_1 \neq \gamma_2$. In this case, the trajectories approach the limit cycle given in (9).

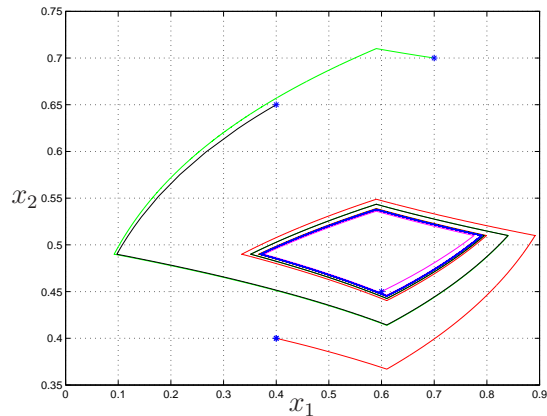


Figure 16: *Solutions approaching the set S with different initial conditions of x_i and fixed parameters. Values of parameters: $\theta_1 = 0.6, \theta_2 = 0.5, \gamma_1 = 5, \gamma_2 = 1, k_1 = 5, k_2 = 1, h_1 = 0.01, h_2 = 0.01$. The blue line is the set S . The symbol $*$ denotes the initial point.*

5 Conclusion

In this paper, a mathematical model of a genetic regulatory network has been developed under the formalism of hybrid dynamical systems. The model presented in this paper permits a quantitative analysis of the cellular protein dynamics under the influence of protein concentration thresholds and initial conditions. The analysis of the hybrid model with two genes determines conditions guaranteeing the existence of solutions, the equilibria of the system, stability properties of the equilibria and its robustness. In particular, we have revealed conditions on the parameters that, when hysteresis is present, the interaction between the concentrations of two proteins leads to oscillatory behavior. Such a behavior is impossible in a two-gene network without hysteresis. The obtained results are an important initial step in the analysis of genetic regulatory networks using hybrid systems theory, which we believe has great potential for the understanding of the complex mechanisms in such networks, in particular, when treated as (larger than two) interconnections of hybrid systems.

References

- [1] H. de Jong, Modeling and simulation of genetic regulatory systems: a literature review, *Journal of Computational Biology* 9 (1) (2002) 67–103.
- [2] M. Chaves, E. D. Sontag, R. Albert, Methods of robustness analysis for boolean models of gene control networks, *Journal of Theoretical Biology* 235 (2005) 431–449.
- [3] L. Glass, L. Kauffman, The logical analysis of continuous, non-linear biochemical control networks, *J. Theor. Biol.* 39 (1) (1973) 103–129.

- [4] E. H. Snoussi, Qualitative dynamics of piecewise-linear differential equations: a discrete mapping approach, *Dynamics and Stability of Systems* 4 (3–4) (1989) 565–583.
- [5] J. L. Gouzé, T. Sari, A class of piecewise linear differential equations arising in biological models, *Dynam. Syst.* 17 (4) (2002) 299–316.
- [6] H. de Jong, J. L. Gouzé, C. Hernandez, M. Page, T. Sari, J. Geiselmann, Hybrid modeling and simulation of genetic regulatory networks: A qualitative approach, *Hybrid Systems: Computation and Control* (2003) 267–282.
- [7] P. Lincoln, A. Tiwari, Symbolic systems biology: Hybrid modeling and analysis of biological networks, *Hybrid Systems: Computation and Control* 2293 (2004) 660–672.
- [8] R. Ghosh, C. J. Tomlin, Lateral inhibition through delta-notch signaling: A piecewise-affine hybrid model, *Hybrid Systems: Computation and Control* 2034 (2001) 232–246.
- [9] V. Noel, D. Grigoriev, S. Vakulenko, O. Radulescu, Hybrid models of the cell cycle molecular machinery, *First International Workshop on Hybrid Systems and Biology* 23 (2012) 88–105.
- [10] S. Huang, Gene expression profiling, genetic networks, and cellular states: an integrating concept for tumorigenesis and drug discovery, *Journal of Molecular Medicine* 77 (1999) 469–480.
- [11] J. Das, M. Ho, J. Zikherman, C. Govern, M. Yang, A. Weiss, A. K. Chakraborty, J. P. Roose, Digital signaling and hysteresis characterize ras activation in lymphoid cells, *Cells* 136 (2009) 337–351.
- [12] B. P. Kramer, M. Fussenegger, Hysteresis in a synthetic mammalian gene network, *Proceedings of the National Academy of Sciences (USA)* 102 (2005) 9517–9522.
- [13] J. Hu, K. R. Qin, C. Xiang, T. H. Lee, Modeling of hysteresis in a mammalian gene regulatory network, *9th Annual International Conference on Computational Systems Bioinformatics* 9 (2010) 50–55.
- [14] L. Qiao, R. B. Nachbar, I. G. Bistability and oscillations in the huang-ferrell model of mapk signalling, *PLoS Computational Biology* 3 (9) (2007) 1819–1826.
- [15] A. Kuznetsov, M. Kaern, N. Kopell, Synchrony in a population of hysteresis-based genetic oscillators, *SIAM Journal of Applied Mathematics* 65 (2) (2004) 392–425.
- [16] Z. Han, L. Yang, W. R. Maclellan, J. N. Weiss, Z. Qu, Hysteresis and cell cycle transitions: How crucial is it?, *Biophysical Journal* 88 (2005) 1626–1634.
- [17] J. Kim, T. G. Kim, S. H. Jung, J. R. Kim, T. Park, P. H. Harrison, K. H. Cho, Evolutionary design principles of modules that control cellular differentiation: consequences for hysteresis and multistationarity, *Bioinformatics* 24 (13) (2008) 1516–1522.
- [18] R. Goebel, R. G. Sanfelice, A. R. Teel, Hybrid dynamical systems, *IEEE Control Systems Magazine* (2009) 28–93.

- [19] T. Mestl, E. Plahte, S. W. Omholt, A mathematical framework for describing and analysing gene regulatory networks, *Journal of Theoretical Biology* 176 (1995) 291–300.
- [20] R. Goebel, R. G. Sanfelice, A. R. Teel, *Hybrid Dynamical Systems: Modeling, Stability, and Robustness*, Princeton University Press, 2012.
- [21] R. G. Sanfelice, R. Goebel, A. R. Teel, Invariance principles for hybrid systems with connections to detectability and asymptotic stability, *IEEE Transactions on Automatic Control* 52 (12) (2007) 2282–2297.
- [22] R. G. Sanfelice, D. A. Copp, P. Nanez, A toolbox for simulation of hybrid systems in Matlab/Simulink: Hybrid Equations (HyEQ) Toolbox, 2013, pp. 101–106.

A

A.1 Proof of Proposition 3.3

We consider the first three cases in Table 1. Since for every point in D , the jump map G changes the value of at least one of the logic variables, we just need to consider the case when $z^* \in C$ to determine isolated equilibrium points z^* . The continuous state x of the system satisfies

$$\dot{x} = \begin{bmatrix} k_1(1 - q_2) - \gamma_1 x_1 \\ k_2 q_1 - \gamma_2 x_2 \end{bmatrix}.$$

To compute equilibrium points, let $F(z^*) = 0$. Then,

$$\begin{bmatrix} k_1(1 - q_2^*) - \gamma_1 x_1^* \\ k_2 q_1^* - \gamma_2 x_2^* \end{bmatrix} = 0$$

and solving for x^* leads to

$$x^* = \begin{bmatrix} \frac{k_1(1 - q_2^*)}{\gamma_1} \\ \frac{k_2 q_1^*}{\gamma_2} \end{bmatrix}.$$

According to the possible values of q^* , all the possibilities of x^* are listed in Table 2. These define vectors z_a^* , z_b^* , z_c^* , and z_d^* , which are to be checked if they satisfy $z^* \in C$.

Table 2: Values of x^* based on different combinations of the values of q^* .

	x^*	q^*
z_a^*	$(\frac{k_1}{\gamma_1}, \frac{k_2}{\gamma_2})$	$q_1^* = 1, q_2^* = 0$
z_b^*	$(0, 0)$	$q_1^* = 0, q_2^* = 1$
z_c^*	$(0, \frac{k_2}{\gamma_2})$	$q_1^* = 1, q_2^* = 1$
z_d^*	$(\frac{k_1}{\gamma_1}, 0)$	$q_1^* = 0, q_2^* = 0$

Similar to C , the jump set D can also be written as $D = \bigcup_{i=1}^4 D_i$, where $D_1 := \{z \in \mathcal{Z} : q_1 = 0, q_2 = 0, x_1 = \theta_1 + h_1, x_2 \leq \theta_2 + h_2\} \cup \{z \in \mathcal{Z} : q_1 = 1, q_2 = 0, x_1 = \theta_1 - h_1, x_2 \leq \theta_2 + h_2\}$, $D_2 := \{z \in \mathcal{Z} : q_1 = 1, q_2 = 1, x_1 = \theta_1 - h_1, x_2 \geq \theta_2 - h_2\} \cup \{z \in \mathcal{Z} : q_1 = 0, q_2 = 1, x_1 = \theta_1 + h_1, x_2 \geq \theta_2 - h_2\}$, $D_3 := \{z \in \mathcal{Z} : q_1 = 1, q_2 = 0, x_1 \geq \theta_1 - h_1, x_2 = \theta_2 + h_2\} \cup \{z \in \mathcal{Z} : q_1 = 1, q_2 = 1, x_1 \geq \theta_1 - h_1, x_2 = \theta_2 - h_2\}$, $D_4 := \{z \in \mathcal{Z} : q_1 = 0, q_2 = 1, x_1 \leq \theta_1 + h_1, x_2 = \theta_2 - h_2\} \cup \{z \in \mathcal{Z} : q_1 = 0, q_2 = 0, x_1 \leq \theta_1 + h_1, x_2 = \theta_2 + h_2\}$. Now, we find the value of $x_1^*, x_2^*, q_1^*, q_2^*$ such that $z^* \in C$.

- Case i : Consider parameters such that $\theta_1 + h_1 < \frac{k_1}{\gamma_1} < \theta_1^{\max}$, $0 < \frac{k_2}{\gamma_2} < \theta_2 + h_2$. Then, it can be checked that

$$z_a^* \in C, z_b^* \notin C, z_c^* \notin C, z_d^* \notin C.$$

Then, z_a^* is an equilibrium point.

- Case *ii*: Consider parameters such that $0 < \frac{k_1}{\gamma_1} < \theta_1 - h_1$, $0 < \frac{k_2}{\gamma_2} < \theta_2 + h_2$. Then, it can be checked that

$$z_a^* \notin C, z_b^* \notin C, z_c^* \notin C, z_d^* \in C.$$

Then, z_d^* is an equilibrium point.

- Case *iii*: Consider parameters such that $\theta_1 + h_1 < \frac{k_1}{\gamma_1} < \theta_1^{\max}$, $\theta_2 + h_2 < \frac{k_2}{\gamma_2} < \theta_2^{\max}$. Then, it can be checked that

$$z_a^* \notin C, z_b^* \notin C, z_c^* \notin C, z_d^* \notin C.$$

- Case *iv*: Consider parameters such that $0 < \frac{k_1}{\gamma_1} < \theta_1 - h_1$, $\theta_2 + h_2 < \frac{k_2}{\gamma_2} < \theta_2^{\max}$. Then, it can be checked that

$$z_a^* \notin C, z_b^* \notin C, z_c^* \notin C, z_d^* \in C.$$

Then, z_d^* is an equilibrium point.

- Case *v*: Consider parameters such that $\theta_1 - h_1 < \frac{k_1}{\gamma_1} < \theta_1 + h_1$, $0 < \frac{k_2}{\gamma_2} < \theta_2 + h_2$. Then, it can be checked that

$$z_a^* \in C, z_b^* \notin C, z_c^* \notin C, z_d^* \in C$$

Then, z_a^* and z_d^* are equilibrium points.

- Case *vi*: Consider parameters such that $\theta_1 - h_1 < \frac{k_1}{\gamma_1} < \theta_1 + h_1$, $\theta_2 + h_2 < \frac{k_2}{\gamma_2} < \theta_2^{\max}$. Then, it can be checked that

$$z_a^* \notin C, z_b^* \notin C, z_c^* \notin C, z_d^* \in C$$

Then, z_d^* is an equilibrium point.

From the properties above, only z_a^* and z_d^* are candidate isolate equilibrium points. We show that the first four cases in Table 1 are equilibrium points of the entire system with $z_1^* = z_a^*$ and $z_2^* = z_d^*$. For case 1, which is when $\theta_1 + h_1 < \frac{k_1}{\gamma_1} < \theta_1^{\max}$, $0 < \frac{k_2}{\gamma_2} < \theta_2 + h_2$, we pick any other $z' \neq z_1^*$. We have that if $z' \in C$ then $F(z') \neq 0$, so z_1^* is the isolated equilibrium point of the system. For case 2, when $0 < \frac{k_1}{\gamma_1} < \theta_1 - h_1$, we pick any other $z' \neq z_2^*$. If $z' \in C$, then $F(z') \neq 0$, so z_2^* is the isolated equilibrium point of the system. For case 3, when $\theta_1 - h_1 < \frac{k_1}{\gamma_1} < \theta_1 + h_1$, $0 < \frac{k_2}{\gamma_2} < \theta_2 + h_2$, we pick any other $z' \neq z_i^*$ for each $i \in \{1, 2\}$. If $z' \in C$, then $F(z') \neq 0$, so z_1^* or z_2^* are the equilibrium points of the entire system. For case 4, when $\theta_1 - h_1 < \frac{k_1}{\gamma_1} < \theta_1 + h_1$, $\theta_2 + h_2 < \frac{k_2}{\gamma_2} < \theta_2^{\max}$ we pick any other $z' \neq z_2^*$. If $z' \in C$, then $F(z') \neq 0$, so z_2^* is the isolated equilibrium point of the system.

We now show that S in (9) is an equilibrium set for case 5 of the parameters in Table 1, namely $\frac{k_1}{\gamma_1} \in (\theta_1 + h_1, \theta_1^{\max})$, $\frac{k_2}{\gamma_2} \in (\theta_2 + h_2, \theta_2^{\max})$. To this end, we establish that for parameters in such range, the logic variables evolve according to the state transition graph in Figure 18. This is due to the system not having an isolated equilibrium point in the flow set C ; see Case *iii* in the proof of Proposition 3.3. Let $Q := \{(0, 0), (0, 1), (1, 0), (1, 1)\}$. The x component of the vector field F satisfies the following properties on the boundary of C .

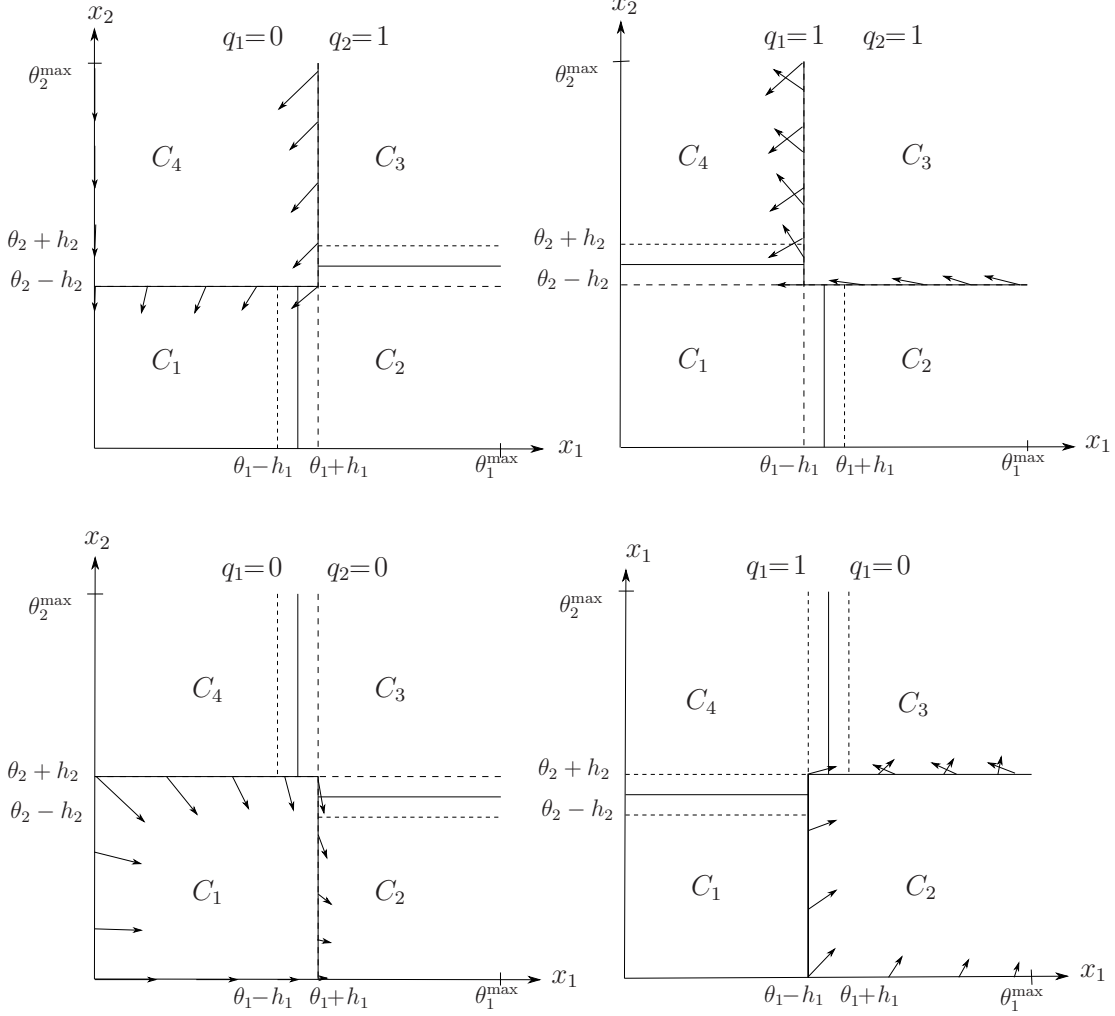


Figure 17: Vector fields on the boundaries of C to case 5 of Table 1.

1. Points on the boundary of C_1 :

- When $x \in \{x : x_1 = 0, 0 \leq x_2 \leq \theta_2 + h_2\}$, the first two components of F define the vector $f_1(x) := \begin{bmatrix} k_1 \\ -\gamma_2 x_2 \end{bmatrix}$. Since $k_1 > 0$, $\gamma_2 > 0$, then $f_1(x)$ points inside of C_1 .
- When $x \in \{x : 0 \leq x_1 \leq \theta_1 + h_1, x_2 = 0\}$, $f_1(x) := \begin{bmatrix} k_1 - \gamma_1 x_1 \\ 0 \end{bmatrix}$. Since $\theta_1 + h_1 < \frac{k_1}{\gamma_1} < \theta_1^{\max}$, then $f_1(x)$ is tangent to the boundary of C_1 .
- When $x \in \{x : 0 \leq x_1 \leq \theta_1 + h_1, x_2 = \theta_2 + h_2\}$, $f_1(x) := \begin{bmatrix} k_1 - \gamma_1 x_1 \\ -\gamma_2(\theta_2 + h_2) \end{bmatrix}$. Since $\theta_1 + h_1 < \frac{k_1}{\gamma_1} < \theta_1^{\max}$, $\gamma_2 > 0$, then $f_1(x)$ points inside of C_1 .
- When $x \in \{x : x_1 = \theta_1 + h_1, 0 \leq x_2 \leq \theta_2 + h_2\}$, $f_1(x) := \begin{bmatrix} k_1 - \gamma_1(\theta_1 + h_1) \\ -\gamma_2 x_2 \end{bmatrix}$.

Since $\theta_1 + h_1 < \frac{k_1}{\gamma_1} < \theta_1^{\max}, \gamma_2 > 0$, then $f_1(x)$ points outside of C_1 .

Then, since there is no isolated equilibrium point in C_1 , trajectories starting in C_1 are such that the x component flow towards $\{x_1 = \theta_1 + h_1, 0 \leq x_2 \leq \theta_2 + h_2\}$.

2. Points on the boundary of C_2 :

- When $x \in \{x : x_1 = \theta_1 - h_1, 0 \leq x_2 \leq \theta_2 + h_2\}$, $f_2(x) := \begin{bmatrix} k_1 - \gamma_1(\theta_1 - h_1) \\ k_2 - \gamma_2 x_2 \end{bmatrix}$. Since $\theta_1 + h_1 < \frac{k_1}{\gamma_1} < \theta_1^{\max}, \theta_2 + h_2 < \frac{k_2}{\gamma_2} < \theta_2^{\max}$, then $f_2(x)$ points inside of C_2 .
- When $x \in \{x : x_1 \geq \theta_1 - h_1, x_2 = 0\}$, $f_2(x) := \begin{bmatrix} k_1 - \gamma_1 x_1 \\ k_2 \end{bmatrix}$. Since $\theta_1 + h_1 < \frac{k_1}{\gamma_1} < \theta_1^{\max}, \theta_2 + h_2 < \frac{k_2}{\gamma_2} < \theta_2^{\max}$, then $f_2(x)$ points inside of C_2 .
- When $x \in \{x : x_1 \geq \theta_1 - h_1, x_2 = \theta_2 + h_2\}$, $f_2(x) := \begin{bmatrix} k_1 - \gamma_1 x_1 \\ k_2 - \gamma_2(\theta_2 + h_2) \end{bmatrix}$. Since $\theta_1 + h_1 < \frac{k_1}{\gamma_1} < \theta_1^{\max}, \theta_2 + h_2 < \frac{k_2}{\gamma_2} < \theta_2^{\max}$, then $f_2(x)$ points outside of C_2 .

Then, since there is no isolated equilibrium point in C_2 , trajectories starting in C_2 are such that the x component flow towards $\{x_1 \geq \theta_1 - h_1, x_2 = \theta_2 + h_2\}$.

3. Points on the boundary of C_3 :

- When $x \in \{x : x_1 \geq \theta_1 - h_1, x_2 = \theta_2 - h_2\}$, $f_3(x) := \begin{bmatrix} -\gamma_1 x_1 \\ k_2 - \gamma_2(\theta_2 - h_2) \end{bmatrix}$. Since $\theta_1 + h_1 < \frac{k_1}{\gamma_1} < \theta_1^{\max}, \theta_2 + h_2 < \frac{k_2}{\gamma_2} < \theta_2^{\max}$, then $f_3(x)$ points inside of C_3 .
- When $x \in \{x : x_1 = \theta_1 - h_1, x_2 \geq \theta_2 - h_2\}$, $f_3(x) := \begin{bmatrix} -\gamma_1(\theta_1 - h_1) \\ k_2 - \gamma_2 x_2 \end{bmatrix}$. Since $\theta_1 + h_1 < \frac{k_1}{\gamma_1} < \theta_1^{\max}, \theta_2 + h_2 < \frac{k_2}{\gamma_2} < \theta_2^{\max}$, then $f_3(x)$ points outside of C_3 .

Then, since there is no isolated equilibrium point in C_3 , the trajectories starting in C_3 have x component that flow towards $\{x_1 = \theta_1 - h_1, x_2 \geq \theta_2 - h_2\}$.

4. Points on the boundary of C_4 :

- When $x \in \{x : x_1 = \theta_1 + h_1, x_2 \geq \theta_2 - h_2\}$, $f_4(x) := \begin{bmatrix} -\gamma_1(\theta_1 + h_1) \\ -\gamma_2 x_2 \end{bmatrix}$. Since $\gamma_1 > 0, \gamma_2 > 0$, then $f_4(x)$ points inside of C_4 .
- When $x \in \{x : x_1 = 0, x_2 \geq \theta_2 - h_2\}$, $f_4(x) := \begin{bmatrix} 0 \\ -\gamma_2 x_2 \end{bmatrix}$. Since $\gamma_2 > 0$, then $f_4(x)$ is tangent to the boundary of C_4 .
- When $x \in \{x : 0 \leq x_1 \leq \theta_1 + h_1, x_2 = \theta_2 - h_2\}$, $f_4(x) := \begin{bmatrix} -\gamma_1 x_1 \\ -\gamma_2(\theta_2 - h_2) \end{bmatrix}$. Since $\gamma_1 > 0, \gamma_2 > 0$, then $f_4(x)$ points outside of the C_4 .

Then, since there is no isolated equilibrium point in C_4 , the trajectories starting in C_4 have x component that flow towards $\{0 \leq x_1 \leq \theta_1 + h_1, x_2 = \theta_2 - h_2\}$.

Combining the above arguments, Figure 18 shows the transition sequence of $q \in Q$ for case 5 in Table 1.

Now, we compute the value of the trajectories as they transition according to the said sequence.

The differential equation for the x components of the continuous dynamics of \mathcal{H} can be evaluated for each possible value of q and written as

$$\dot{x} = K(q) - \Gamma x, \quad (34)$$

where $\Gamma = \begin{bmatrix} \gamma_1 & 0 \\ 0 & \gamma_2 \end{bmatrix}$ and $K : Q \rightarrow \mathbb{R}^{2 \times 1}$ is given by

$$K(q) = \begin{cases} \begin{bmatrix} k_1 \\ 0 \end{bmatrix} & \text{if } q = (0, 0), \\ \begin{bmatrix} 0 \\ 0 \end{bmatrix} & \text{if } q = (0, 1), \\ \begin{bmatrix} k_1 \\ k_2 \end{bmatrix} & \text{if } q = (1, 0), \\ \begin{bmatrix} 0 \\ k_2 \end{bmatrix} & \text{if } q = (1, 1). \end{cases}$$

Restricted to C , (34) is a linear time-invariant system. For any initial condition $z(0, 0) = [x(0, 0)^\top \ q(0, 0)^\top]^\top \in C$, the unique solution to (34) for each $t \geq 0$, up to the first jump, is given by

$$x(t, 0) = u(q(0, 0)) + \exp(-\Gamma t)(x(0, 0) - u(q(0, 0))), \quad (35)$$

where $u(q) = \Gamma^{-1}K(q)$ for each $q \in Q$.

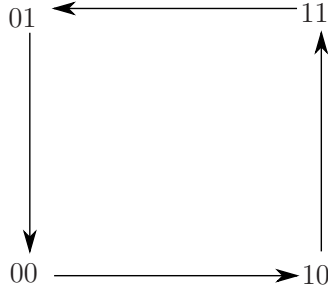


Figure 18: *Transition graph of $q \in Q$.*

For the initial value of q given by $q^0 = \begin{bmatrix} 0 \\ 0 \end{bmatrix}$ and the initial value of x given by

$$x(0, 0) = p_0 = \begin{bmatrix} p_0(1) \\ \theta_2 - h_2 \end{bmatrix},$$

the solution to (34) is given by

$$x(t, 0) = \begin{bmatrix} u_1 - (u_1 - x_1(0, 0)) \exp(-\gamma_1 t) \\ x_2(0, 0) \exp(-\gamma_2 t) \end{bmatrix}$$

where $u_1 = \frac{k_1}{\gamma_1}$. Since $K((0,0)) = \begin{bmatrix} k_1 \\ 0 \end{bmatrix}$ implies that $u(q) = \begin{bmatrix} \frac{k_1}{\gamma_1} \\ 0 \end{bmatrix}$. Note that $x_2(t,0)$ decreases to zero in C_1 and that $x_1(t,0)$ is increasing in C_1 , reaching the threshold value $x_1 = \theta_1 + h_1$ at $t'_1 = \ln \left[\frac{u_1 - x_1(0,0)}{u_1 - (\theta_1 + h_1)} \right]^{\frac{1}{\gamma_1}}$. A jump of q to $\begin{bmatrix} 1 \\ 0 \end{bmatrix}$ occurs at $t = t_1, j = 0$.

After the jump, the initial value of x is p_1 , where

$$p_1 = \begin{bmatrix} \theta_1 + h_1 \\ p_0(2) \left(\frac{u_1 - (\theta_1 + h_1)}{u_1 - p_0(1)} \right)^{\frac{\gamma_2}{\gamma_1}} \end{bmatrix}. \quad (36)$$

Proceeding similarly as when the initial state was p_0 , we obtain the following expressions for p_2, p_3 , and p_4 :

$$\begin{aligned} p_2 &= \begin{bmatrix} u_1 - (u_1 - p_1(1)) \left(\frac{u_2 - p_2(2)}{u_2 - p_1(2)} \right)^{\frac{\gamma_1}{\gamma_2}} \\ \theta_2 + h_2 \end{bmatrix}, \\ p_3 &= \begin{bmatrix} \theta_1 - h_1 \\ u_2 - (u_2 - p_2(2)) \left(\frac{p_3(1)}{p_2(1)} \right)^{\frac{\gamma_2}{\gamma_1}} \end{bmatrix}, \quad p_4 = \begin{bmatrix} p_3(1) \left(\frac{p_4(2)}{p_3(2)} \right)^{\frac{\gamma_1}{\gamma_2}} \\ \theta_2 - h_2 \end{bmatrix}, \end{aligned} \quad (37)$$

where $u_2 = \frac{k_2}{\gamma_2}$. Also, similarly, we have the expression for t'_2, t'_3, t'_4 :

$$t'_2 = \ln \left[\frac{u_2 - p_1(2)}{u_2 - (\theta_2 + h_2)} \right]^{\frac{1}{\gamma_2}}, \quad t'_3 = \ln \left[\frac{p_2(1)}{\theta_1 - h_1} \right]^{\frac{1}{\gamma_1}}, \quad t'_4 = \ln \left[\frac{p_3(2)}{\theta_2 - h_2} \right]^{\frac{1}{\gamma_2}}.$$

Then, the period of the limit cycle is given by $T = t'_1 + t'_2 + t'_3 + t'_4$. Note that $t_1 = t'_1$, $t_2 = t'_1 + t'_2$, $t_3 = t'_1 + t'_2 + t'_3$ and $t_4 = t'_1 + t'_2 + t'_3 + t'_4$, where t_1, t_2, t_3 and t_4 define the jump times $(t_1, 0)$, $(t_2, 1)$, $(t_3, 2)$, and $(t_4, 3)$.

Now, we define the map $\rho : [0, \theta_1^{\max}] \rightarrow \mathbb{R}$ as

$$\rho(r) = \rho_4 \circ \rho_3 \circ \rho_2 \circ \rho_1(r),$$

where

$$\begin{aligned} \rho_1(r) &= (\theta_2 - h_2) \left(\frac{u_1 - (\theta_1 + h_1)}{u_1 - r} \right)^{\frac{\gamma_2}{\gamma_1}}, \\ \rho_2(r) &= u_1 - (u_1 - (\theta_1 + h_1)) \left(\frac{u_2 - (\theta_2 + h_2)}{u_2 - r} \right)^{\frac{\gamma_1}{\gamma_2}}, \\ \rho_3(r) &= u_2 - (u_2 - (\theta_2 + h_2)) \left(\frac{\theta_1 - h_1}{r} \right)^{\frac{\gamma_2}{\gamma_1}}, \\ \rho_4(r) &= (\theta_1 - h_1) \left(\frac{\theta_2 - h_2}{r} \right)^{\frac{\gamma_1}{\gamma_2}}. \end{aligned}$$

Then, r such that

$$\rho(r) = r$$

defines $p_0(1)$.

Then, combining the above expressions, we obtain (10)-(13). Finally, using (35), the set S is constructed by combining the x components of the (unique) solutions between these points. Since each piece of the x component corresponding to a constant value of q is a solution to a linear system, this set of points has the property that, from every point in it, the only existing solution from that point stays in the set, i.e., the set is strongly forward invariant.

A.2 Proof of Proposition 3.1

To verify the sufficient conditions for the existence of nontrivial solutions from an initial point in $C \cup D$, it is enough to show that $F(z) \in T_C(z)$ for every $z \in C \setminus D$ in the boundary of C (the **(VC)** condition holds for every point in the interior of C .)

Next, we consider each possible case.

1. Let $z \in C_1 \setminus D_1 = \{z : q_1 = 0, q_2 = 0, 0 \leq x_1 < \theta_1 + h_1, 0 \leq x_2 \leq \theta_2 + h_2\}$. Let

$$\begin{aligned} T_{C_1}^1(z) &= \{w \in \mathbb{R}^2 : w_1 \geq 0, w_2 \leq 0\}, \\ T_{C_1}^2(z) &= \{w \in \mathbb{R}^2 : w_1 \geq 0\}, \\ T_{C_1}^3(z) &= \{w \in \mathbb{R}^2 : w_1 \geq 0, w_2 \geq 0\}, \\ T_{C_1}^4(z) &= \{w \in \mathbb{R}^2 : w_2 \geq 0\}, \\ T_{C_1}^5(z) &= \{w \in \mathbb{R}^2 : w_1 \leq 0, w_2 \geq 0\}, \\ T_{C_1}^6(z) &= \{w \in \mathbb{R}^2 : w_1 \leq 0\}, \\ T_{C_1}^7(z) &= \{w \in \mathbb{R}^2 : w_1 \leq 0, w_2 \leq 0\}, \\ T_{C_1}^8(z) &= \{w \in \mathbb{R}^2 : w_2 \leq 0\}. \end{aligned}$$

Then, the tangent cone of C_1 at points $z = (x, q)$ is given as follows:

- For $x \in \{x : x_1 = 0, x_2 = \theta_2 + h_2\}$, $T_{C_1}(z) = T_{C_1}^1(z)$,
- For $x \in \{x : x_1 = 0, 0 < x_2 < \theta_2 + h_2\}$, $T_{C_1}(z) = T_{C_1}^2(z)$.
- For $x \in \{x : x_1 = 0, x_2 = 0\}$, $T_{C_1}(z) = T_{C_1}^3(z)$.
- For $x \in \{0 < x_1 < \theta_1 + h_1, x_2 = 0\}$, $T_{C_1}(z) = T_{C_1}^4(z)$,
- For $x \in \{x : x_1 = \theta_1 + h_1, x_2 = 0\}$, $T_{C_1}(z) = T_{C_1}^5(z)$.
- For $x \in \{x_1 = \theta_1 + h_1, 0 < x_2 < \theta_2 + h_2\}$, $T_{C_1}(z) = T_{C_1}^6(z)$,
- For $x \in \{x_1 = \theta_1 + h_1, x_2 = \theta_2 + h_2\}$, $T_{C_1}(z) = T_{C_1}^7(z)$,
- For $x \in \{0 < x_1 < \theta_1 + h_1, x_2 = \theta_2 + h_2\}$, $T_{C_1}(z) = T_{C_1}^8(z)$.

Now, we check the vector field F on the boundary of C_1 away from D_1 .

- When $x \in \{x : x_1 = 0, 0 \leq x_2 \leq \theta_2 + h_2\}$, $f_1(x) := \begin{bmatrix} k_1 \\ -\gamma_2 x_2 \end{bmatrix}$. Since $k_1 > 0$, $f_1(x)$ points inside of C_1 .

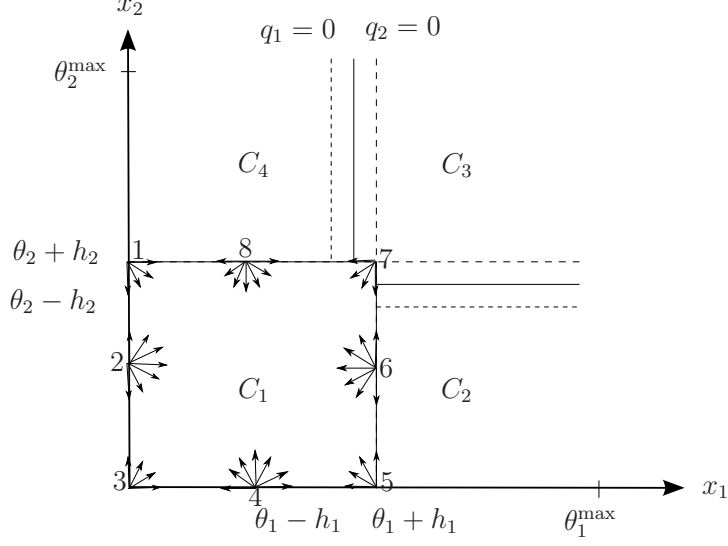


Figure 19: *Tangent cones on the boundaries of C_1 .*

- When $x \in \{x : 0 \leq x_1 \leq \theta_1 + h_1, x_2 = 0\}$, $f_1(x) := \begin{bmatrix} k_1 - \gamma_1 x_1 \\ 0 \end{bmatrix}$. Then, $f_1(x)$ is tangent to the boundary of C_1 .

Then, $F(z) \in T_{C_1}$ holds, implying that **(VC)** holds at each point $z \in C_1 \setminus D_1$.

2. Let $z \in C_2 \setminus D_2 = \{z : q_1 = 1, q_2 = 0, x_1 \geq \theta_1 - h_1, 0 \leq x_2 < \theta_2 + h_2\}$. Let

$$\begin{aligned}
 T_{C_2}^1(z) &= \{w \in \mathbb{R}^2 : w_2 \geq 0\}, \\
 T_{C_2}^2(z) &= \{w \in \mathbb{R}^2 : w_1 \geq 0, w_2 \geq 0\}, \\
 T_{C_2}^3(z) &= \{w \in \mathbb{R}^2 : w_1 \geq 0\}, \\
 T_{C_2}^4(z) &= \{w \in \mathbb{R}^2 : w_1 \leq 0, w_2 \geq 0\}, \\
 T_{C_2}^5(z) &= \{w \in \mathbb{R}^2 : w_2 \leq 0\}.
 \end{aligned}$$

Then, the tangent cone of C_2 is given by as follows:

- For $x \in \{x : x_1 > \theta_1 - h_1, x_2 = 0\}$, $T_{C_2}(z) = T_{C_2}^1(z)$,
- For $x \in \{x : x_1 = \theta_1 - h_1, x_2 = 0\}$, $T_{C_2}(z) = T_{C_2}^2(z)$.
- For $x \in \{x : x_1 = \theta_1 - h_1, 0 \leq x_2 \leq \theta_2 + h_2\}$, $T_{C_2}(z) = T_{C_2}^3(z)$.
- For $x \in \{x_1 = \theta_1 - h_1, x_2 = \theta_2 + h_2\}$, $T_{C_2}(z) = T_{C_2}^4(z)$,
- For $x \in \{x : x_1 > \theta_1 - h_1, x_2 = \theta_2 + h_2\}$, $T_{C_2}(z) = T_{C_2}^5(z)$.

Figure 20 depicts the tangent cones on the boundaries of C_2 .

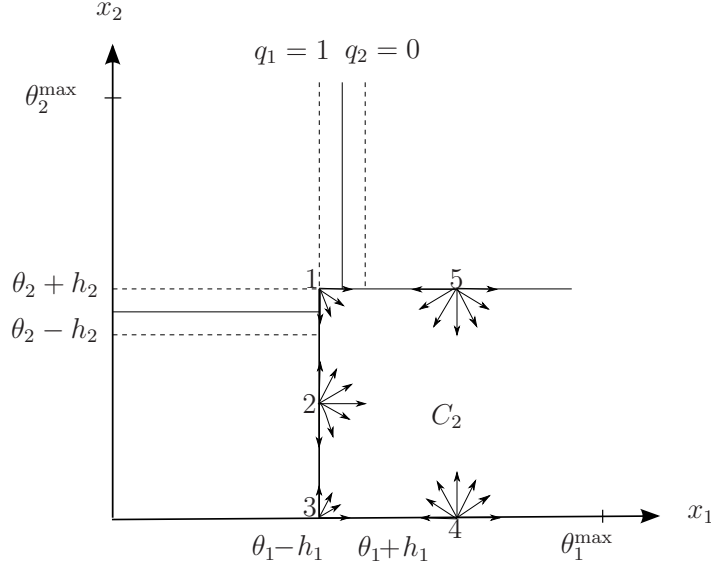


Figure 20: *The tangent cone of C_2 when $\theta_1 + h_1 < \frac{k_1}{\gamma_1} < \theta_1^{\max}, 0 < \frac{k_2}{\gamma_2} < \theta_2 + h_2$.*

Now, we check the vector field F on the boundary of C_2 away from D_2 .

- When $x \in \{x : x_1 \geq \theta_1 - h_1, x_2 = 0\}$, $f_2(x) := \begin{bmatrix} k_1 - \gamma_1 x_1 \\ k_2 \end{bmatrix}$. Since $k_2 > 0$, we have that $f_2(x)$ points inside of C_2 .

Then, $F(z) \in T_{C_2}(z)$ holds, implying that **(VC)** holds at each point $z \in C_2 \setminus D_2$.

3. Let $z \in C_3 \setminus D_3 = \{z : q_1 = 1, q_2 = 1, x_1 > \theta_1 - h_1, x_2 > \theta_2 - h_2\}$.

Since there are no points in the boundary of C_3 that are not in D_3 , **(VC)** holds for free.

4. Let $z \in C_4 \setminus D_4 = \{z : q_1 = 0, q_2 = 1, 0 \leq x_1 \leq \theta_1 + h_1, x_2 > \theta_2 - h_2\}$. Let

$$\begin{aligned} T_{C_4}^1(z) &= \{w \in \mathbb{R}^2 : w_1 \leq 0\}, \\ T_{C_4}^2(z) &= \{w \in \mathbb{R}^2 : w_1 \leq 0, w_2 \geq 0\}, \\ T_{C_4}^3(z) &= \{w \in \mathbb{R}^2 : w_2 \geq 0\}, \\ T_{C_4}^4(z) &= \{w \in \mathbb{R}^2 : w_1 \geq 0, w_2 \geq 0\}, \\ T_{C_4}^5(z) &= \{w \in \mathbb{R}^2 : w_1 \geq 0\}. \end{aligned}$$

Then, the tangent cone of C_4 is given by as follows:

- For $x \in \{x : x_1 = \theta_1 + h_1, x_2 > \theta_2 - h_2\}$, $T_{C_4}(z) = T_{C_4}^1(z)$,
- For $x \in \{x : x_1 = \theta_1 + h_1, x_2 = \theta_2 - h_2\}$, $T_{C_4}(z) = T_{C_4}^2(z)$.

- For $x \in \{x : 0 < x_1 < \theta_1 + h_1, x_2 = \theta_2 - h_2\}$, $T_{C_4}(z) = T_{C_4}^3(z)$.
- For $x \in \{x_1 = 0, x_2 = \theta_2 - h_2\}$, $T_{C_4}(z) = T_{C_4}^4(z)$,
- For $x \in \{x : x_1 = 0, x_2 > \theta_2 - h_2\}$, $T_{C_4}(z) = T_{C_4}^5(z)$.

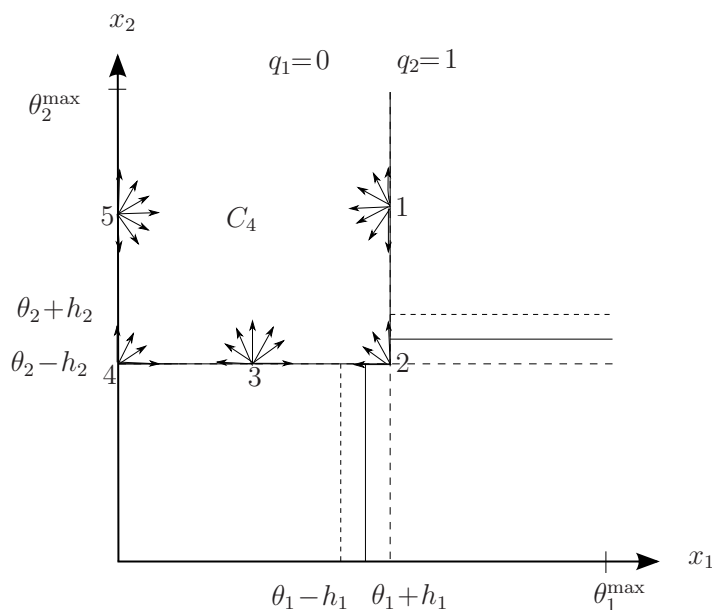


Figure 21: *Tangent cones on the boundaries of C_4 .*

Now, we check the vector field F on the boundary of C_4 away from D_4 .

- When $x \in \{x : x_1 = 0, x_2 \geq \theta_2 - h_2\}$, $f_4(x) := \begin{bmatrix} 0 \\ -\gamma_2 x_2 \end{bmatrix}$, and $f_4(x)$ is tangent to the boundary of C_4 . Then, $F(z) \in T_{C_4}(z)$ holds at each point $z \in C_4 \setminus D_4$.

Combining the above arguments, for each case in Table 1, **(VC)** holds and nontrivial solutions to \mathcal{H} in (8) exist.

Since f_i is linear, every solution to $\dot{z} = F(z)$ subject to $z \in C$ does not escape to infinity by flowing. Then, condition 2) below (VC) does not hold. Since $G(D) \subset C \cup D$, then condition 3) therein does not hold either.

Finally, every solution is not Zeno, since at most after the second jump, every solution needs to flow (linearly) from the value after the jump, which is given by G , for at least $2 \min\{h_1, h_2\}$ in the x_1 or in the x_2 direction (for certain initial conditions, e.g., $z(0, 0) = [\theta_1 - h_1, \theta_2 - h_2, 1, 1]$, solutions jump twice consecutively, and after that, flow for the said amount).

A.3 Proof of Proposition 3.5

Note that when $\theta_1 + h_1 < \frac{k_1}{\gamma_1} < \theta_1^{max}, 0 < \frac{k_2}{\gamma_2} < \theta_2 + h_2, q_1 = 1, q_2 = 0,$

$$\begin{aligned} 0 = \dot{x}_1 = k_1 - \gamma_1 x_1 &\Rightarrow k_1 - \gamma_1 x_1 = 0 \Rightarrow x_1^* = \frac{k_1}{\gamma_1} \\ 0 = \dot{x}_2 = k_2 - \gamma_2 x_2 &\Rightarrow k_2 - \gamma_2 x_2 = 0 \Rightarrow x_2^* = \frac{k_2}{\gamma_2}, \end{aligned}$$

from where we have $z_1^* = [x^{*\top} \ 1 \ 0]^\top \in C_2$. Now, change to e coordinates given by

$$e_1 = x_1 - x_1^*, \quad e_2 = x_2 - x_2^*.$$

We have that

$$\begin{aligned} \dot{e}_1 &= \dot{x}_1 - \dot{x}_1^* = k_1 - \gamma_1 x_1 - 0 = k_1 - \gamma_1(e_1 + x_1^*) \\ &= k_1 - \gamma_1 e_1 - k_1 = -\gamma_1 e_1, \\ \dot{e}_2 &= \dot{x}_2 - \dot{x}_2^* = k_2 - \gamma_2 x_2 - 0 = k_2 - \gamma_2(e_2 + x_2^*) \\ &= k_2 - \gamma_2 e_2 - k_2 = -\gamma_2 e_2. \end{aligned}$$

Then, the x component of $\dot{z} = F(z)$ leads to

$$\dot{e} = \begin{bmatrix} -\gamma_1 & 0 \\ 0 & -\gamma_2 \end{bmatrix} e.$$

Then, since γ_1 and γ_2 are positive, we have that z_1^* is (exponentially) stable – this property can be easily certified with the Lyapunov function $V(e) = e^\top e$.

Now we check the vector fields of boundaries of C_2 (see Figure 22).

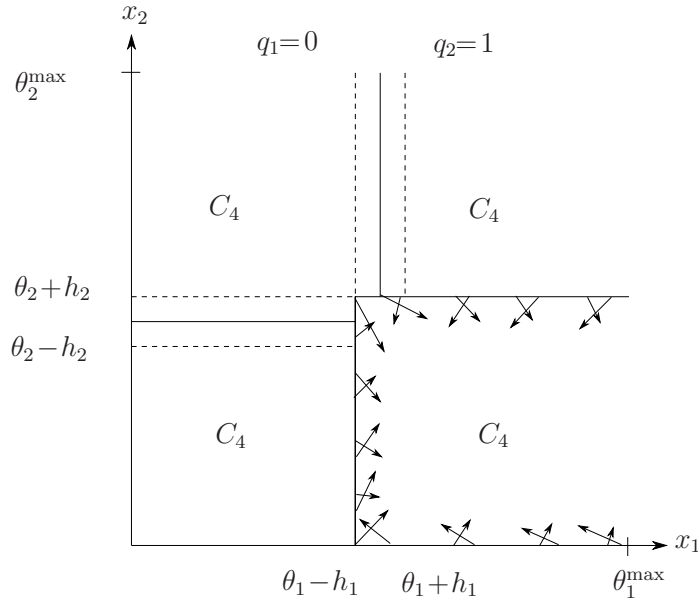


Figure 22: The vector fields on the boundaries of C_2 when $\theta_1 + h_1 < \frac{k_1}{\gamma_1} < \theta_1^{max}, 0 < \frac{k_2}{\gamma_2} < \theta_2 + h_2$.

- When $x \in \{x : x_1 = \theta_1 - h_1, 0 \leq x_2 \leq \theta_2 + h_2\}$, $f_2(x) = \begin{bmatrix} k_1 - \gamma_1(\theta_1 - h_1) \\ k_2 - \gamma_2 x_2 \end{bmatrix}$. Since $\theta_1 + h_1 < \frac{k_1}{\gamma_1} < \theta_1^{max}$, $0 < \frac{k_2}{\gamma_2} < \theta_2 + h_2$, we have that $f_2(x)$ points inside of C_2 .
- When $x \in \{x : x_1 \geq \theta_1 - h_1, x_2 = \theta_2 + h_2\}$, $f_2(x) = \begin{bmatrix} k_1 - \gamma_1 x_1 \\ k_2 - \gamma_2(\theta_2 + h_2) \end{bmatrix}$. Since $\theta_1 + h_1 < \frac{k_1}{\gamma_1} < \theta_1^{max}$, $0 < \frac{k_2}{\gamma_2} < \theta_2 + h_2$, we have that $f_2(x)$ points inside of C_2 .
- When $x \in \{x : x_1 \geq \theta_1 - h_1, x_2 = 0\}$, $f_2(x) = \begin{bmatrix} k_1 - \gamma_1 x_1 \\ k_2 \end{bmatrix}$. Since $\theta_1 + h_1 < \frac{k_1}{\gamma_1} < \theta_1^{max}$, $k_2 > 0$, we have that $f_2(x)$ points inside of C_2 .

Then, once a trajectory enters or starts in C_2 , it will stay and never leave C_2 , i.e., the set C_2 is forward invariant. As a consequence, since the equilibrium point z_1^* belongs to C_2 , every trajectory starting from or reaching C_2 converges to z_1^* .

Global asymptotic stability follows since for every initial condition $z(0, 0) \in (C \cup D) \setminus C_2$, solutions reach C_2 in finite time. To establish this property, we check the vector field of the system on the boundary of each set C_i , for each $i \in \{1, 3, 4\}$.

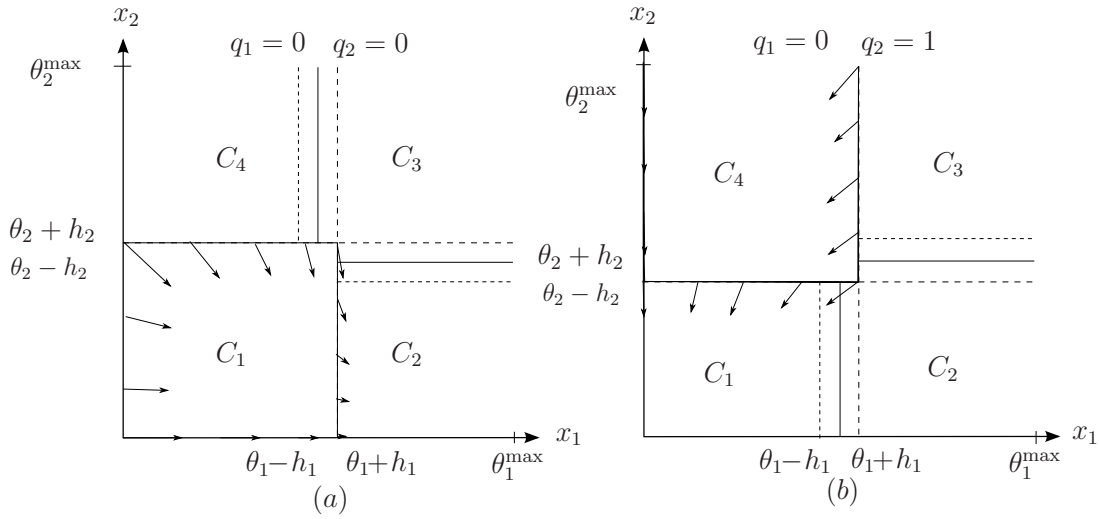


Figure 23: Vector fields at the boundaries of C_1, C_4 , when $\theta_1 + h_1 < \frac{k_1}{\gamma_1} < \theta_1^{max}$, $0 < \frac{k_2}{\gamma_2} < \theta_2 + h_2$. (a) The vector field at the boundaries of C_1 , (b) The vector field of the boundaries of C_4 .

- For initial points $z(0, 0) \in C_1$ (see Figure 23(a)), when $x \in \{x : 0 \leq x_1 < \theta_1 + h_1, x_2 = \theta_2 + h_2\}$, $f_1(x) = \begin{bmatrix} k_1 - \gamma_1 x_1 \\ -\gamma_2(\theta_2 + h_2) \end{bmatrix}$. Since $\theta_1 + h_1 < \frac{k_1}{\gamma_1} < \theta_1^{max}$, $0 < \frac{k_2}{\gamma_1} < \theta_2 + h_2$ we have that $f_1(x)$ points inside C_1 . When $x \in \{x : x_1 = \theta_1 + h_1, 0 \leq x_2 \leq \theta_2 + h_2\}$, $f_1(x) = \begin{bmatrix} k_1 - \gamma_1(\theta_1 + h_1) \\ -\gamma_2 x_2 \end{bmatrix}$. Since $\frac{k_1}{\gamma_1} > \theta_1 + h_1$, we have that $f_1(x)$ points outside C_1 . Thus, for every point $z \in C_1$, x_1 reaches $\theta_1 + h_1$ since there is no equilibrium point in C_1 for this range of parameters. Then, a jump occurs. After the jump, the solution belongs to C_2 .

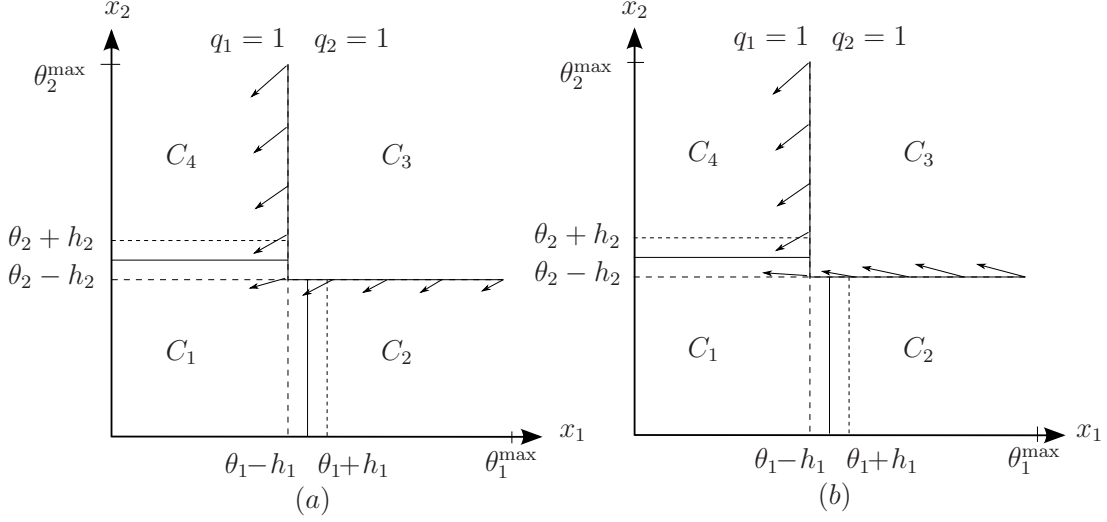


Figure 24: The vector field at the boundaries of C_3 , when $\theta_1 + h_1 < \frac{k_1}{\gamma_1} < \theta_1^{max}, \frac{k_2}{\gamma_2} < \theta_2 + h_2$.
(a) Case $\frac{k_2}{\gamma_2} < \theta_2 - h_2$, (b) Case $\theta_2 - h_2 < \frac{k_2}{\gamma_2} < \theta_2 + h_2$

- For each initial point $z(0,0) \in C_4$ (see Figure 23(b)), when $x \in \{x : 0 \leq x_1 < \theta_1 + h_1, x_2 = \theta_2 - h_2\}$, $f_4(x) = \begin{bmatrix} -\gamma_1 x_1 \\ -\gamma_2(\theta_2 - h_2) \end{bmatrix}$. Then, we have that $f_4(x)$ points outside C_4 and every solution leaves C_4 by jumping into C_1 when x_1 reaches $\theta_1 - h_1$, from where it will enter C_2 in finite time. When $x \in \{x : x_1 = \theta_1 + h_1, x_2 > \theta_2 - h_2\}$, $f_4(x) = \begin{bmatrix} -\gamma_1(\theta_1 + h_1) \\ -\gamma_2 x_2 \end{bmatrix}$. Then, we have that $f_4(x)$ points inside C_4 . Then, for every initial condition $z(0,0) \in C_4$, solutions will reach C_2 in finite time.
- For every initial point $z(0,0) \in C_3$ (see Figure 24(a)), if $0 < \frac{k_2}{\gamma_2} < \theta_2 - h_2$, when $x \in \{x : x_1 \geq \theta_1 - h_1, x_2 = \theta_2 - h_2\}$, $f_3(x) = \begin{bmatrix} -\gamma_1 x_1 \\ k_2 - \gamma_2(\theta_2 - h_2) \end{bmatrix}$. We have that $f_3(x)$ points outside of C_3 . When $x \in \{x_1 = \theta_1 - h_1, x_2 \geq \theta_2 - h_2\}$, we have $f_3(x) = \begin{bmatrix} -\gamma_1(\theta_1 - h_1) \\ k_2 - \gamma_2 x_2 \end{bmatrix}$, which points outside C_3 . If $\theta_2 - h_2 < \frac{k_2}{\gamma_2} < \theta_2 + h_2$ (see Figure 24(b)), when $x \in \{x : \theta_1 - h_1 < x_1 < \theta_1^{max}, x_2 = \theta_2 - h_2\}$, $f_3(x) = \begin{bmatrix} -\gamma_1 x_1 \\ k_2 - \gamma_2(\theta_2 - h_2) \end{bmatrix}$ points inside C_3 . When $x \in \{x : x_1 = \theta_1 - h_1, x_2 \geq \theta_2 - h_2\}$, $f_3(x) = \begin{bmatrix} -\gamma_1(\theta_1 - h_1) \\ k_2 - \gamma_2 x_2 \end{bmatrix}$ points outside C_3 . Then, from $z(0,0) \in C_3$, solutions will leave C_3 and jump into C_4 or C_2 . Using the arguments above, solutions will enter inside of C_2 in finite time.

From the arguments above, when $\theta_1 + h_1 < \frac{k_1}{\gamma_1} < \theta_1^{max}$, $0 < \frac{k_2}{\gamma_2} < \theta_2 + h_2$, the equilibrium point z_1^* is globally asymptotically stable.

For case 2 in Table 1, it can be proven that z_2^* is globally asymptotically stable.

Note that when $q_1 = 0, q_2 = 0$, $0 < \frac{k_1}{\gamma_1} < \theta_1 - h_1$,

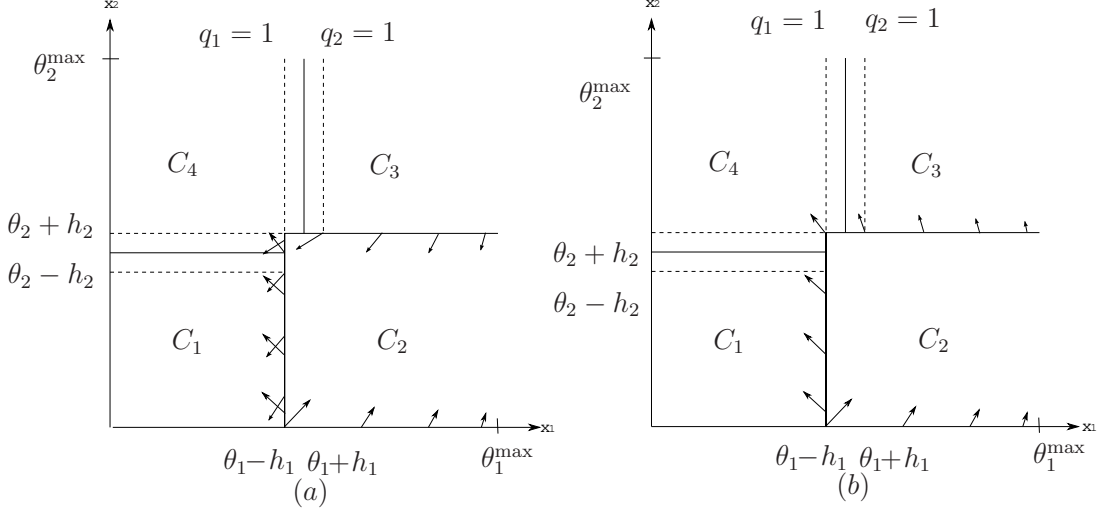


Figure 25: *The vector field at the boundaries of C_2 , when $0 < \frac{k_1}{\gamma_1} < \theta_1 + h_1$. (a) Case $\frac{k_2}{\gamma_2} < \theta_2 + h_2$, (b) Case $\frac{k_2}{\gamma_2} > \theta_2 + h_2$.*

$$\begin{aligned} 0 = \dot{x}_1 = k_1 - \gamma_1 x_1 &\Rightarrow k_1 - \gamma_1 x_1 = 0 \Rightarrow x_1^* = \frac{k_1}{\gamma_1} \\ 0 = \dot{x}_2 = \gamma_2 x_2 &\Rightarrow -\gamma_2 x_2 = 0 \Rightarrow x_2^* = 0, \end{aligned}$$

from where we have $z_2^* = [x^{*\top} \ 0 \ 0]^\top \in C_1$. Now, change to e coordinates given by

$$e_1 = x_1 - x_1^*, \quad e_2 = x_2 - x_2^*.$$

We have that

$$\begin{aligned} \dot{e}_1 &= \dot{x}_1 - \dot{x}_1^* = k_1 - \gamma_1 x_1 - 0 = k_1 - \gamma_1(e_1 + x_1^*) \\ &= k_1 - \gamma_1 e_1 - k_1 = -\gamma_1 e_1, \\ \dot{e}_2 &= \dot{x}_2 = k_2 - \gamma_2 x_2 = k_2 - \gamma_2(e_2 + x_2^*) \\ &= k_2 - \gamma_2 e_2 - k_2 = -\gamma_2 e_2. \end{aligned}$$

Then, the x component of $\dot{z} = F(z)$ becomes

$$\dot{e} = \begin{bmatrix} -\gamma_1 & 0 \\ 0 & -\gamma_2 \end{bmatrix} e.$$

Then, since γ_1 and γ_2 are positive, we have that z_2^* is stable (this property can be certified with the Lyapunov function $V(e) = e^\top e$).

Now we check the vector fields on the boundaries of C_1 (see Figure 26).

- When $x \in \{x : x_1 = \theta_1 + h_1, 0 \leq x_2 \leq \theta_2 + h_2\}$, $f_1(x) = \begin{bmatrix} k_1 - \gamma_1(\theta_1 + h_1) \\ -\gamma_2 x_2 \end{bmatrix}$. Since $0 < \frac{k_1}{\gamma_1} < \theta_1 - h_1$, we have that $f_1(x)$ points inside C_1 .

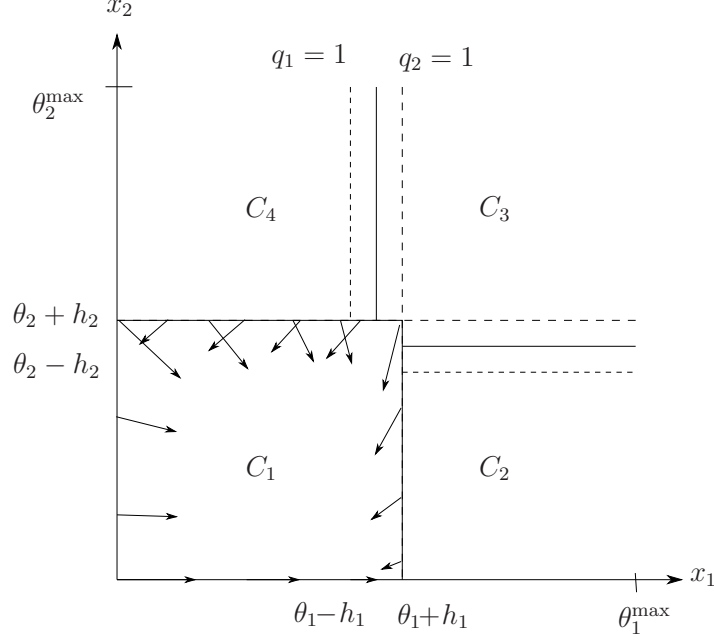


Figure 26: The vector field at the boundaries of C_1 , when $0 < \frac{k_1}{\gamma_1} < \theta_1 - h_1$.

- When $x \in \{x : 0 \leq x_1 \leq \theta_1 + h_1, x_2 = \theta_2 + h_2\}$, $f_1(x) = \begin{bmatrix} k_1 - \gamma_1 x_1 \\ -\gamma_2(\theta_2 + h_2) \end{bmatrix}$. Since $0 < \frac{k_1}{\gamma_1} < \theta_1 - h_1$, we have that $f_1(x)$ points inside C_1 .
- When $x \in \{x : 0 \leq x_1 \leq \theta_1 + h_1, x_2 = 0\}$, $f_1(x) = \begin{bmatrix} k_1 - \gamma_1 x_1 \\ 0 \end{bmatrix}$. $f_1(x)$ is tangent to the boundary of C_1 .
- When $x \in \{x : x_1 = 0, 0 \leq x_2 \leq \theta_2 + h_2\}$, $f_1(x) = \begin{bmatrix} k_1 \\ -\gamma_2 x_2 \end{bmatrix}$. Since $k_1 > 0$, we have that $f_1(x)$ points inside C_1 .

Then, every trajectory that enters or starts from C_1 will stay or never leave C_1 . Then, the set C_1 is forward invariant.

Since the equilibrium point z_2^* belongs to C_1 , every trajectory that reaches or starts from C_1 converges to z_2^* .

Global asymptotic stability follows since for every initial condition $z(0, 0) \in (C \cup D) \setminus C_1$, solutions reach C_1 in finite time. To establish this property, we check the vector field of the system on the boundary of each set C_i , for each $i \in \{2, 3, 4\}$.

- For initial points $z(0, 0) \in C_2$:
 - if $\frac{k_2}{\gamma_2} < \theta_2 + h_2$ (see Figure 25(a)), when $x \in \{x : x_1 = \theta_1 - h_1, 0 \leq x_2 \leq \theta_2 + h_2\}$, $f_2(x) = \begin{bmatrix} k_1 - \gamma_1(\theta_1 - h_1) \\ k_2 - \gamma_2 x_2 \end{bmatrix}$. Since $0 < \frac{k_1}{\gamma_1} < \theta_1 - h_1$, we have that $f_2(x)$ points outside of C_2 . When $x \in \{x : x_1 > \theta_1 - h_1, x_2 = \theta_2 + h_2\}$, $f_2(x) =$

$\begin{bmatrix} k_1 - \gamma_1 x_1 \\ k_2 - \gamma_2(\theta_2 + h_2) \end{bmatrix}$. Since $0 < \frac{k_1}{\gamma_1} < \theta_1 - h_1$, we have that $f_2(x)$ points inside of C_2 .

Since there is no equilibrium point in C_2 for this range of parameters and the dynamics of x are linear, x_1 reaches $\theta_1 - h_1$ for every point $z \in C_2$. Then, a jump occurs. After the jump, the solution belongs to C_1 .

- If $\frac{k_2}{\gamma_2} > \theta_2 + h_2$ (see Figure 25(b)), when $x \in \{x : x_1 = \theta_1 - h_1, 0 \leq x_2 \leq \theta_2 + h_2\}$, $f_2(x) = \begin{bmatrix} k_1 - \gamma_1(\theta_1 - h_1) \\ k_2 - \gamma_2 x_2 \end{bmatrix}$. Since $0 < \frac{k_1}{\gamma_1} < \theta_1 - h_1$, we have that $f_2(x)$ points outside of C_2 . When $x \in \{x : x_1 \geq \theta_1 - h_1, x_2 = \theta_2 + h_2\}$, $f_1(x) = \begin{bmatrix} k_1 - \gamma_1 x_1 \\ k_2 - \gamma_2(\theta_2 + h_2) \end{bmatrix}$. Since $0 < \frac{k_1}{\gamma_1} < \theta_1 - h_1$, we have that $f_2(x)$ points outside C_2 .

Then, from $z(0, 0) \in C_2$, solutions will leave C_2 and jump into C_1 or C_3 .

- For every initial point $z(0, 0) \in C_3$:

- if $\frac{k_2}{\gamma_2} < \theta_2 - h_2$, when $x \in \{x : x_1 \geq \theta_1 - h_1, x_2 = \theta_2 - h_2\}$ (see similar case shown in Figure 24(a)), $f_3(x) = \begin{bmatrix} -\gamma_1 x_1 \\ k_2 - \gamma_2(\theta_2 - h_2) \end{bmatrix}$. We have that $f_3(x)$ points outside of C_3 . When $x \in \{x : x_1 = \theta_1 - h_1, x_2 \geq \theta_2 - h_2\}$, we have $f_3(x) = \begin{bmatrix} -\gamma_1(\theta_1 - h_1) \\ k_2 - \gamma_2 x_2 \end{bmatrix}$, which points outside of C_3 .
- If $\theta_2 - h_2 < \frac{k_2}{\gamma_2} < \theta_2 + h_2$ (see similar case shown in Figure 24(b)), when $x \in \{x : x_1 = \theta_1 - h_1, x_2 \geq \theta_2 - h_2\}$, $f_3(x) = \begin{bmatrix} -\gamma_1(\theta_1 - h_1) \\ k_2 - \gamma_2 x_2 \end{bmatrix}$ points outside of C_3 . When $x \in \{x : x_1 > \theta_1 - h_1, x_2 = \theta_2 - h_2\}$, $f_3(x) = \begin{bmatrix} -\gamma_1 x_1 \\ k_2 - \gamma_2(\theta_2 - h_2) \end{bmatrix}$. We have that $f_3(x)$ points inside of C_3 .

Then, from $z(0, 0) \in C_3$, solutions will leave C_3 and jump into C_4 or C_2 .

- For each initial point $z(0, 0) \in C_4$ (see similar case shown in Figure 23(b)), when $x \in \{x : 0 \leq x_1 < \theta_1 + h_1, x_2 = \theta_2 - h_2\}$, $f_4(x) = \begin{bmatrix} -\gamma_1 x_1 \\ -\gamma_2(\theta_2 - h_2) \end{bmatrix}$. Then, we have that $f_4(x)$ points outside C_4 and every solution leaves C_4 by jumping into C_1 . When $x \in \{x : x_1 = \theta_1 + h_1, x_2 > \theta_2 - h_2\}$, $f_4(x) = \begin{bmatrix} -\gamma_1(\theta_1 + h_1) \\ -\gamma_2 x_2 \end{bmatrix}$. Then, we have that $f_4(x)$ points inside C_4 . Then, for every initial condition $z(0, 0) \in C_4$, solutions will reach C_1 in finite time.

From the above analysis, we have that: 1) from C_2 trajectories go to either C_1 or C_3 ; 2) from C_3 trajectories go to either C_1 or C_4 ; 3) from C_4 trajectories go to C_1 .

Then, trajectories eventually enter C_1 , which, using the arguments above, implies that the equilibrium point z_2^* is globally asymptotically stable.

Similarly, for case 4 in Table 1, it can be proven that z_2^* is globally asymptotically stable. Since stability of z_2^* was proven in the proof of case 2 in Table 1, now we check the vector fields on the boundaries of C_1 when $\theta_1 - h_1 < \frac{k_1}{\gamma_1} < \theta_1 + h_1$, $\theta_2 + h_2 < \frac{k_2}{\gamma_2} < \theta_2^{max}$ (see Figure 27).

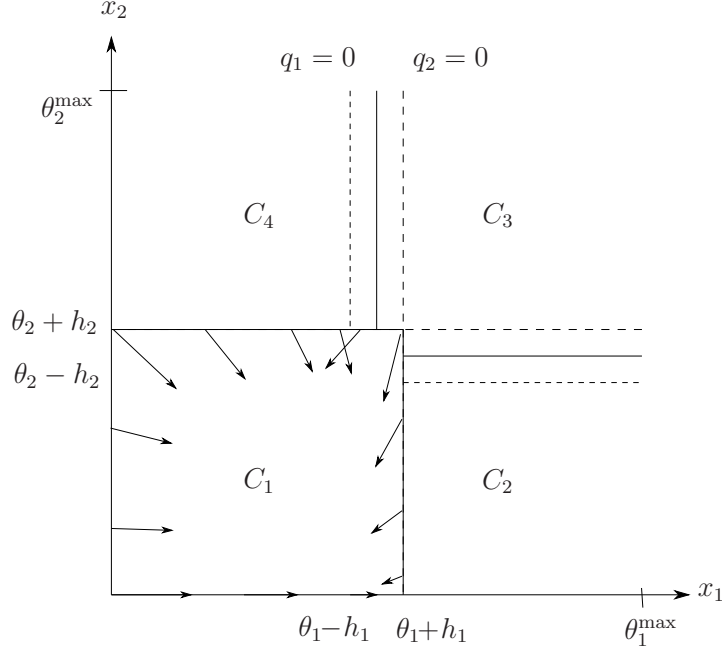


Figure 27: *The vector field at the boundaries of C_1 , when $\theta_1 - h_1 < \frac{k_1}{\gamma_1} < \theta_1 + h_1$, $\theta_2 + h_2 < \frac{k_2}{\gamma_2} < \theta_2^{max}$.*

- When $x \in \{x : x_1 = \theta_1 + h_1, 0 \leq x_2 \leq \theta_2 + h_2\}$, $f_1(x) = \begin{bmatrix} k_1 - \gamma_1(\theta_1 + h_1) \\ -\gamma_2 x_2 \end{bmatrix}$. Since $\theta_1 - h_1 < \frac{k_1}{\gamma_1} < \theta_1 + h_1$, we have that $f_1(x)$ points inside C_1 .
- When $x \in \{x : 0 \leq x_1 \leq \theta_1 + h_1, x_2 = \theta_2 + h_2\}$, $f_1(x) = \begin{bmatrix} k_1 - \gamma_1 x_1 \\ -\gamma_2(\theta_2 + h_2) \end{bmatrix}$. Since $\theta_1 - h_1 < \frac{k_1}{\gamma_1} < \theta_1 + h_1$, $\theta_2 + h_2 < \frac{k_2}{\gamma_2} < \theta_2^{max}$, we have that $f_1(x)$ points inside C_1 .
- When $x \in \{x : 0 \leq x_1 \leq \theta_1 + h_1, x_2 = 0\}$, $f_1(x) = \begin{bmatrix} k_1 - \gamma_1 x_1 \\ 0 \end{bmatrix}$. $f_1(x)$ is tangent to the boundary of C_1 .
- When $x \in \{x : x_1 = 0, 0 \leq x_2 \leq \theta_2 + h_2\}$, $f_1(x) = \begin{bmatrix} k_1 \\ -\gamma_2 x_2 \end{bmatrix}$. Since $k_1 > 0$, we have that $f_1(x)$ points inside C_1 .

Then, every trajectory that enters or starts from C_1 will stay or never leave C_1 . Then, the set C_1 is forward invariant.

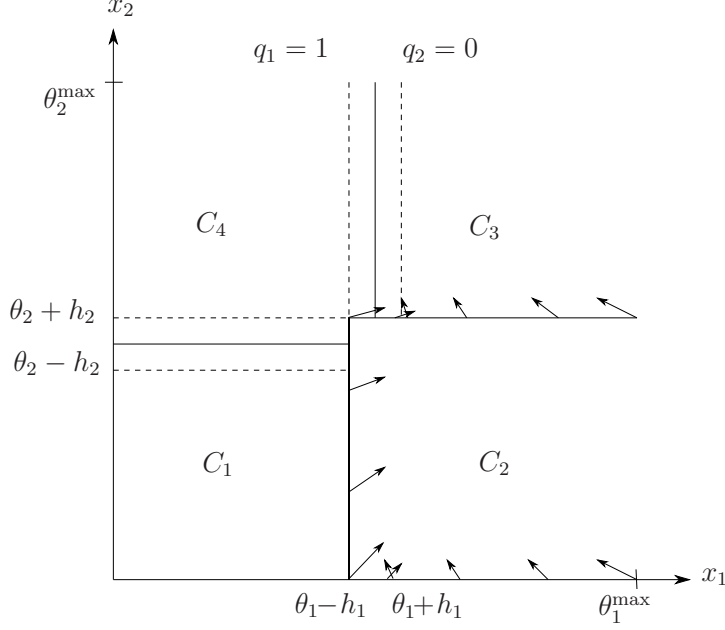


Figure 28: The vector field at the boundaries of C_2 , when $\theta_1 - h_1 < \frac{k_1}{\gamma_1} < \theta_1 + h_1$, $\theta_2 + h_2 < \frac{k_2}{\gamma_2} < \theta_2^{\max}$.

Since the equilibrium point z_2^* belongs to C_1 , every trajectory that reaches or starts from C_1 converges to z_2^* .

Global asymptotic stability follows since for every initial condition $z(0, 0) \in (C \cup D) \setminus C_1$, solutions reach C_1 in finite time. To establish this property, we check the vector field of the system on the boundary of each set C_i , for each $i \in \{2, 3, 4\}$.

- For initial points $z(0, 0) \in C_2$: When $x \in \{x : x_1 = \theta_1 - h_1, 0 \leq x_2 < \theta_2 + h_2\}$ (see Figure 28), $f_2(x) = \begin{bmatrix} k_1 - \gamma_1(\theta_1 - h_1) \\ k_2 - \gamma_2 x_2 \end{bmatrix}$. Since $\theta_1 - h_1 < \frac{k_1}{\gamma_1} < \theta_1 + h_1$, we have that $f_2(x)$ points inside of C_2 . When $x \in \{x : x_1 \geq \theta_1 - h_1, x_2 = \theta_2 + h_2\}$, $f_2(x) = \begin{bmatrix} k_1 - \gamma_1 x_1 \\ k_2 - \gamma_2(\theta_2 + h_2) \end{bmatrix}$. Since $\theta_1 - h_1 < \frac{k_1}{\gamma_1} < \theta_1 + h_1$, $\theta_2 + h_2 < \frac{k_2}{\gamma_2} < \theta_2^{\max}$, we have that $f_2(x)$ points outside of C_2 .

Since there is no equilibrium point in C_2 for this range of parameters and the dynamics of x are linear, x_2 reaches $\theta_2 + h_2$ for every point $z \in C_2$.

Then, from $z(0, 0) \in C_2$, solutions will leave C_2 and jump into C_3 .

- For every initial point $z(0, 0) \in C_3$: (see Figure 29) when $x \in \{x : x_1 = \theta_1 - h_1, x_2 \geq \theta_2 - h_2\}$, since $\theta_1 - h_1 < \frac{k_1}{\gamma_1} < \theta_1 + h_1$, $f_3(x) = \begin{bmatrix} -\gamma_1(\theta_1 - h_1) \\ k_2 - \gamma_2 x_2 \end{bmatrix}$ points outside of C_3 . When $x \in \{x : x_1 > \theta_1 - h_1, x_2 = \theta_2 - h_2\}$, $f_3(x) = \begin{bmatrix} -\gamma_1 x_1 \\ k_2 - \gamma_2(\theta_2 - h_2) \end{bmatrix}$. Since $\theta_1 - h_1 < \frac{k_1}{\gamma_1} < \theta_1 + h_1$, we have that $f_3(x)$ points inside of C_3 . Then, from $z(0, 0) \in C_3$, solutions will leave C_3 and jump into C_4 .

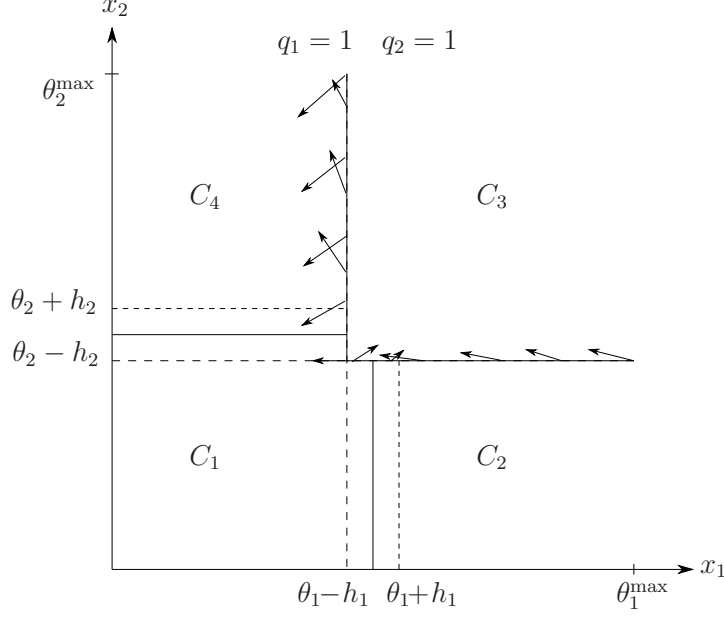


Figure 29: The vector field at the boundaries of C_3 , when $\theta_1 - h_1 < \frac{k_1}{\gamma_1} < \theta_1 + h_1$, $\theta_2 + h_2 < \frac{k_2}{\gamma_2} < \theta_2^{\max}$.

- For each initial point $z(0, 0) \in C_4$: (see similar case shown in Figure 23(b)) when $x \in \{x : 0 \leq x_1 < \theta_1 + h_1, x_2 = \theta_2 - h_2\}$, since $\theta_1 - h_1 < \frac{k_1}{\gamma_1} < \theta_1 + h_1$, $f_4(x) = \begin{bmatrix} -\gamma_1 x_1 \\ -\gamma_2(\theta_2 - h_2) \end{bmatrix}$. Then, we have that $f_4(x)$ points outside C_4 and every solution leaves C_4 by jumping into C_1 . When $x \in \{x : x_1 = \theta_1 + h_1, x_2 > \theta_2 - h_2\}$, $f_4(x) = \begin{bmatrix} -\gamma_1(\theta_1 + h_1) \\ -\gamma_2 x_2 \end{bmatrix}$. Then, we have that $f_4(x)$ points inside C_4 . Then, for every initial condition $z(0, 0) \in C_4$, solutions will reach C_1 in finite time.

From the above analysis, we have that: 1) from C_2 trajectories go to C_3 ; 2) from C_3 trajectories go to C_4 ; 3) from C_4 trajectories go to C_1 .

Then, trajectories eventually enter C_1 , which, using the arguments above, implies that the equilibrium point z_2^* is globally asymptotically stable.

A.4 Proof of Proposition 3.6

For case 3, when $\theta_1 - h_1 < \frac{k_1}{\gamma_1} < \theta_1 + h_1$, $\frac{k_2}{\gamma_2} < \theta_2 + h_2$, z_1^* and z_2^* are located in the region noted as C' in Figure 30.

For an initial point $z(0, 0) \in C_2$, we check the vector fields on the boundaries of C_2 (see Figure 31(a)).

- When $x \in \{x : x_1 = \theta_1 - h_1, 0 \leq x_2 \leq \theta_2 + h_2\}$, $f_2(x) = \begin{bmatrix} k_1 - \gamma_1(\theta_1 - h_1) \\ k_2 - \gamma_2 x_2 \end{bmatrix}$. Since $\theta_1 - h_1 < \frac{k_1}{\gamma_1} < \theta_1 + h_1, 0 < \frac{k_2}{\gamma_2} < \theta_2 + h_2$, we have that $f_2(x)$ points inside of C_2 .

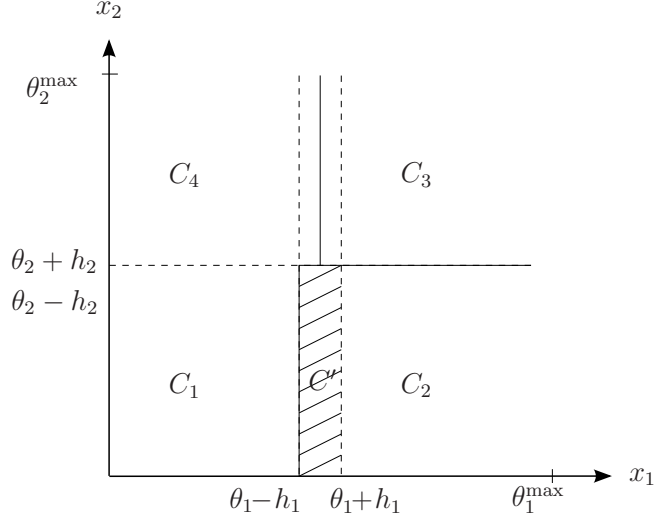


Figure 30: *Region C' given by the overlap between C_1 and C_2 when projected onto the x component.*

- When $x \in \{x : x_1 \geq \theta_1 - h_1, x_2 = \theta_2 + h_2\}$, $f_2(x) = \begin{bmatrix} k_1 - \gamma_1 x_1 \\ k_2 - \gamma_2(\theta_2 + h_2) \end{bmatrix}$. Since $\theta_1 - h_1 < \frac{k_1}{\gamma_1} < \theta_1 + h_1$, $0 < \frac{k_2}{\gamma_2} < \theta_2 + h_2$, we have that $f_2(x)$ points inside of C_2 .
- When $x \in \{x : x_1 \geq \theta_1 - h_1, x_2 = 0\}$, $f_2(x) = \begin{bmatrix} k_1 - \gamma_1 x_1 \\ k_2 \end{bmatrix}$. Since $\theta_1 - h_1 < \frac{k_1}{\gamma_1} < \theta_1 + h_1, k_2 > 0$, we have that $f_2(x)$ points inside of C_2 .

Then, once a trajectory enters or starts from C_2 , it will stay or never leave C_2 . Then, the set C_2 is forward invariant. Since the equilibrium point z_1^* belongs to C_2 , every trajectory reaching or starting from C_2 converges to z_1^* .

For $z(0, 0) \in C_1$, we check the vector fields on the boundaries of C_1 (see Figure 31(b)).

- When $x \in \{x : x_1 = \theta_1 + h_1, 0 \leq x_2 \leq \theta_2 + h_2\}$, $f_1(x) = \begin{bmatrix} k_1 - \gamma_1(\theta_1 + h_1) \\ -\gamma_2 x_2 \end{bmatrix}$. Since $\theta_1 - h_1 < \frac{k_1}{\gamma_1} < \theta_1 + h_1$, we have that $f_1(x)$ points inside C_1 .
- When $x \in \{x : 0 \leq x_1 \leq \theta_1 + h_1, x_2 = \theta_2 + h_2\}$, $f_1(x) = \begin{bmatrix} k_1 - \gamma_1 x_1 \\ -\gamma_2(\theta_2 + h_2) \end{bmatrix}$. Since $\theta_1 - h_1 < \frac{k_1}{\gamma_1} < \theta_1 + h_1$, we have that $f_1(x)$ points inside C_1 .
- When $x \in \{x : 0 \leq x_1 \leq \theta_1 + h_1, x_2 = 0\}$, $f_1(x) = \begin{bmatrix} k_1 - \gamma_1(\theta_1 + h_1) \\ 0 \end{bmatrix}$. $f_1(x)$ is tangent to the boundary of C_1 .
- When $x \in \{x : x_1 = 0, 0 \leq x_2 \leq \theta_2 + h_2\}$, $f_1(x) = \begin{bmatrix} k_1 \\ -\gamma_2 x_2 \end{bmatrix}$. Since $k_1 > 0$, we have that $f_1(x)$ points inside C_1 .

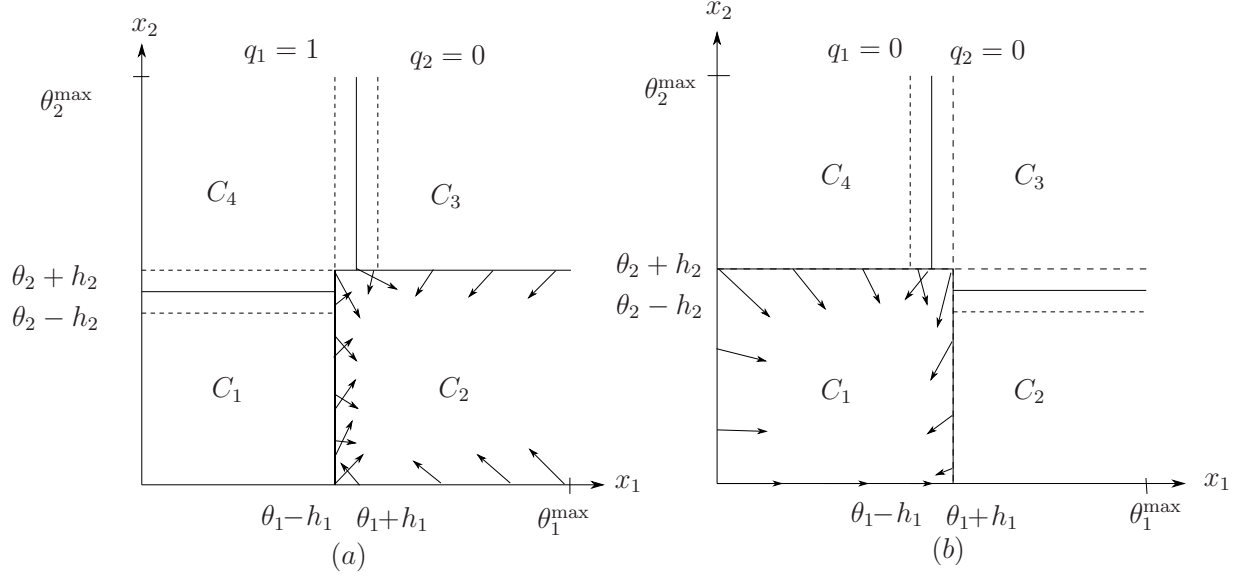


Figure 31: when $\theta_1 - h_1 < \frac{k_1}{\gamma_1} < \theta_1 + h_1, 0 < \frac{k_2}{\gamma_2} < \theta_2 + h_2$: (a) the vector field at the boundaries of C_2 , (b) the vector field at the boundaries of C_1 .

Then, once a trajectory enters or starts from C_1 , it will stay or never leave C_1 . Then, the set C_1 is forward invariant. Since the equilibrium point z_2^* belongs to C_1 , every trajectory reaching or starting from C_1 converges to z_2^* .

For initial points in C_4 , the vector field of the boundary at C_4 is shown in Figure 23 (b). When $x \in \{x : 0 < x_1 < \theta_1 + h_1, x_2 = \theta_2 - h_2\}$, $f_4(x) = \begin{bmatrix} -\gamma_1 x_1 \\ -\gamma_2(\theta_2 - h_2) \end{bmatrix}$. Then, we have that $f_4(x)$ points outside C_4 and every solution leaves C_4 by jumping into C_1 . Then, for every initial condition $z(0, 0) \in C_4$, solutions will reach C_1 in finite time. As $z_2^* \in C_1$, so the trajectory will stay in C_1 and converge to z_2^* .

If $z(0, 0) \in C_3$, the vector field at the boundary of C_3 is similar as that shown in Figure 24.

1. If the parameters are in the range of $\theta_1 - h_1 < \frac{k_1}{\gamma_1} < \theta_1 + h_1, 0 < \frac{k_2}{\gamma_2} < \theta_2 - h_2$ (see similar case shown in Figure 24(a)), when $x \in \{x : \theta_1 - h_1 < x_1 < \theta_1^{\max}, x_2 = \theta_2 - h_2\}$, $f_3(x) = \begin{bmatrix} -\gamma_1 x_1 \\ k_2 - \gamma_2(\theta_2 - h_2) \end{bmatrix}$. We have that $f_3(x)$ points outside of C_3 . When $x \in \{x : x_1 = \theta_1 - h_1, x_2 \geq \theta_2 - h_2\}$, we have $f_3(x) = \begin{bmatrix} -\gamma_1(\theta_1 - h_1) \\ k_2 - \gamma_2 x_2 \end{bmatrix}$, which points outside C_3 . Depending on which jump set the solution hits, two possibilities of the equilibrium points exist.

- If the trajectory hits the set $x \in \{x : x_1 = \theta_1 - h_1, x_2 > \theta_2 - h_2\}$, which leads to an update of q_1 , the solution will jump into C_4 . For this case, the trajectory will reach C_1 in finite time and converge to z_2^* .
- If the trajectory hits the set $x \in \{x : x_1 > \theta_1 - h_1, x_2 = \theta_2 - h_2\}$, q_2 is updated to 0 from 1, the trajectory will enter C_2 , and converge to the equilibrium point z_1^* , which is inside of C_2 .

2. If the parameters are in the range of $\theta_1 - h_1 < \frac{k_1}{\gamma_1} < \theta_1 + h_1, \theta_2 - h_2 < \frac{k_2}{\gamma_2} < \theta_2 + h_2$ (see similar case shown in Figure 24(b)), when $x \in \{x : x_1 > \theta_1 + h_1, x_2 = \theta_2 - h_2\}$, $f_3(x) = \begin{bmatrix} -\gamma_1 x_1 \\ k_2 - \gamma_2(\theta_2 - h_2) \end{bmatrix}$. We have that $f_3(x)$ points inside of C_3 . When $x \in \{x : x_1 = \theta_1 - h_1, x_2 \geq \theta_2 - h_2\}$, we have $f_3(x) = \begin{bmatrix} -\gamma_1(\theta_1 - h_1) \\ k_2 - \gamma_2 x_2 \end{bmatrix}$, which points outside of C_3 . Thus, when the trajectory hits the set $\{x : x_1 = \theta_1 - h_1, x_2 > \theta_2 - h_2\}$, a jump will occur, the solution will jump into C_4 and finally enter C_1 and converge to z_2^* .